Desalination

A scalable dual-layer PAN/SAN nanofibrous membrane for treatment of saline oily water using membrane distillation

--Manuscript Draft--

Manuscript Number:	DES-D-23-00351R2
Article Type:	VSI:MD and MCr
Section/Category:	Membrane desalination processes
Keywords:	hydrophilicity; Underwater superoleophobicity; Hot-pressing; Dual-layer; DCMD.
Corresponding Author:	Ali Sallakh Niknejad University of Cincinnati UNITED STATES
First Author:	Ali Sallakh Niknejad
Order of Authors:	Ali Sallakh Niknejad
	Ali Kargari
	Mahsa Namdari
	Mohammad Pishnamazi
	Masoud Barani
	Esmaeil Ranjbari
	Reza Sallakhniknezhad
	Saeed Bazgir
	Mohsen Rasouli
	Drew C Mcavoy
Abstract:	Single-layer hydrophobic membranes are prone to fouling while subjected to a feed containing hydrophobic contaminants. In this study, using the green solvent Dimethyl sulfoxide (DMSO), dual-layer nanofibrous poly-acrylonitrile (PAN)/styrene-acrylonitrile (SAN) membranes were fabricated using the highly productive electroblowing process. Then through a simple hot-pressing process, the desirable hydrophilicity was achieved for PAN/SAN membrane. The water contact angle (WCA) for the top layer fell from 112.2 ± 1° to 37.5 ± 1° after hot-pressing, while the WCA for the bottom layer decreased slightly from 147.1 ± 1° to 142.3 ± 1°. Moreover, an underwater oil contact angle (UOCA) of 158.1 ± 1° was achieved for the PAN/SAN membrane. Direct contact membrane distillation (DCMD) tests were performed for synthetic saline water and synthetic saline oily water. While the permeate flux dropped for the single-layer SAN membrane, the dual-layer PAN/SAN membrane, due to underwater superoleophobicity, achieved a stable permeate flux for 24 h with a nearly complete salt rejection (>99.9%). This study addresses the pore wetting and declines in the permeate flux of the membrane distillation (MD) application in the treatment of saline oily water by implementing scalable, cost-efficient, and eco-friendly approaches.
Suggested Reviewers:	Hamidreza Sanaeepur h-sanaeepur@araku.ac.ir
	Hyunsik Kim kim4hk@mail.uc.edu
	Salman Ahmadipouya Salman.ahmadipouya@uconn.edu
Opposed Reviewers:	
Response to Reviewers:	

A scalable dual-layer PAN/SAN nanofibrous membrane for treatment of saline oily water using membrane distillation

Ali Sallakh Niknejad [*1,4], Ali Kargari [*2], Mahsa Namdari [3], Mohammad Pishnamazi [1], Masoud Barani [4], Esmaeil Ranjbari [4], Reza Sallakhniknezhad [5], Saeed Bazgir [4,6], Mohsen Rasouli [7], Drew McAvoy [1]

[1] *Department of Chemical and Environmental Engineering, University of Cincinnati, Cincinnati, Ohio, USA*

[2] *Membrane Processes Research Laboratory (MPRL), Department of Chemical Engineering, Amirkabir University of Technology (Tehran Polytechnic), Tehran, Iran*

[3] *Department of Chemical Engineering, Amirkabir University of Technology, Tehran, Iran*

[4] *Nano polymer Research Laboratory (NPRL), Science and Research Branch, Islamic Azad University, Tehran, Iran*

[5] *School of Mechanical Engineering, Beijing Institute of Technology, Beijing, China*

[6] *Department of Polymer Engineering, Petroleum and Chemical Engineering Faculty, Science and Research Branch, Islamic Azad University, Tehran, Iran*

[7] *SEM Lab, Central Laboratory, Amirkabir University of Technology, Tehran, Iran*

Corresponding authors:

Ali Sallakh Niknejad (Email: *aliniknejad1991@gmail.com*; *sallakai@mail.uc.edu*)

Ali Kargari (Tel/fax: +98-21-66405847; E-mail: *kargari@aut.ac.ir*; *ali_kargari@yahoo.com*)

Abstract

Single-layer hydrophobic membranes are prone to fouling while subjected to a feed containing hydrophobic contaminants. In this study, using the green solvent Dimethyl sulfoxide (DMSO), dual-layer nanofibrous poly-acrylonitrile (PAN)/styrene-acrylonitrile (SAN) membranes were fabricated using the highly productive electroblowing process. Then through a simple hot-pressing process, the desirable hydrophilicity was achieved for PAN/SAN membrane. The water contact angle (WCA) for the top layer fell from 112.2 ± 1° to 37.5 ± 1° after hot-pressing, while the WCA for the bottom layer decreased slightly from 147.1 ± 1° to 142.3 ± 1°. Moreover, an underwater oil contact angle (UOCA) of 158.1 ± 1° was achieved for the PAN/SAN membrane. Direct contact membrane distillation (DCMD) tests were performed for synthetic saline water and synthetic saline oily water. While the permeate flux dropped for the single-layer SAN membrane, the dual-layer PAN/SAN membrane, due to underwater superoleophobicity, achieved a stable permeate flux for 24 h with a nearly complete salt rejection (>99.9%). This study addresses the pore wetting and declines in the permeate flux of the membrane distillation (MD) application in the treatment of saline oily water by implementing scalable, cost-efficient, and eco-friendly approaches.

Keywords: Hydrophilicity; Underwater superoleophobicity; Hot-pressing; Dual-layer; DCMD.

Contents

1. Introduction 3
2. Experimental 5
2.1. Materials and chemicals 5
2.2. Membrane fabrication process 6
2.3. Characterization 6
2.4. DCMD process 7
3. Results and discussion 8
3.1. Morphology 8
3.2. Porosity and thickness 11
3.3. Wettability 12

3.4. DCMD 16
4. Conclusion 20
Declaration of competing interest 20
Acknowledgment 20
Appendix A. Supplementary data 21
References 21

1. Introduction

Saline wastewater production has increased in recent decades due to considerable development in varied industries [1,2]. Wastewater treatment can be done using methods like physicochemical processes, aerobic treatment, anaerobic digestion, and membrane separation technologies [3-6]. Considering membrane-based separation, the membrane distillation (MD) process has been regarded as a next-generation, sustainable approach to treating hypersaline waters. The MD is a non-isothermal process that uses a porous hydrophobic membrane to direct hot water vapor to produce pure water [7,8]. Interestingly, MD can make full use of inexpensive heat resources to supply clean water and due to its operational condition, it will not be influenced by the quality of wastewater, making it a sought-after technology for desalination and wastewater treatment [9-13].

Surface fouling and pore wetting are however the downsides of the MD process due to the complex composition of hypersaline wastewaters [14]. In general, membrane performance can be detrimentally affected by fouling [15-17]. Severe reduction in membrane permeation because of foulant accumulation on/in the membrane can be followed by pore wetting and worsening of treated water quality [18,19]. Although the MD process experiences lower fouling compared to the pressure-driven membrane processes, the MD membranes are vulnerable to oil due to strong hydrophobic-hydrophobic interaction [20]. Low-surface-energy materials like surfactants can also increase the pore wetting of the MD membrane. These contaminants can easily invade the

78 membrane pores and render the membrane more hydrophilic which will lead to the failure in
79 rejecting salts [21-23].

80 To tackle the problem of traditional MD membranes, the concept of dual-layer structure
81 including hydrophilic/hydrophobic design has been proposed to reduce fouling and wetting
82 [24,25]. As dual-layer structures have two layers with hydrophilic and hydrophobic characteristics,
83 researchers called them the Janus membranes after the imaginary Greek god with two faces [26].
84 The hydrophilic layer of a dual-layer structure can be fabricated by coating with hydrophilic
85 materials [27], electrospinning [28], electrospraying [29], and film casting using non-solvent-
86 induced phase separation (NIPS) [30] to form a hydrophilic or even superhydrophilic top layer
87 with superior underwater oil repellency. The hydrophobic/superhydrophobic or even omniphobic
88 support layer can also be applied to reject salts to avoid pore wetting, while the hydrophilic top
89 layer reduces fouling.

90 The robustness of the top layer is of vital importance in using dual-layer membranes.
91 Delamination or removal of the top layer during the MD process allows oil droplets to attach to
92 the membrane surface and reduce the permeate flux [31]. It also causes a severe reduction in
93 rejection because of pore wetting. Another issue is the environmental concern for using
94 hydrophilic materials, fluoroalkyl silanes, and also the complexity of the membrane fabrication
95 process. From an industrial point of view, a fabrication process should be time-efficient and as
96 simple as possible with a considerably lower production cost for both applied materials and the
97 fabrication process.

98 In this study, a practical dual-layer structure was fabricated using inexpensive
99 polyacrylonitrile (PAN) and styrene-acrylonitrile (SAN) polymers. To make the fabrication
100 process more productive and less time-consuming, a modified version of the conventional

electrospinning, electroblowing process was used. The electroblowing or air-assisted electrospinning process makes use of dry airflow to boost the fiber production rate [32,33]. The PAN polymer and its nanofibers are intrinsically hydrophilic but not hydrophilic enough to be used as a decent top layer for reducing oil fouling. The surface hydrophilicity was impressively improved using a fast-hot-pressing process. The fabricated structure turned from a spongy and soft structure to a dense and firm structure that: 1) reduced the chance of top-layer detachment during the direct contact MD (DCMD) process, 2) decreased the hydrophobicity of the surface to sufficiently reduce underwater interaction between membrane surface and oil droplets, 3) minimized the carbon footprint resulted from the application of different materials that are currently applied to make more hydrophilic surfaces. The membrane fabrication process was also eco-friendly because of the use of dimethyl sulfoxide (DMSO) as the solvent during the electroblowing process. To our knowledge, this is the first report of constructing an underwater superoleophobic and in-air highly hydrophilic dual-layer structure for the MD process using a straightforward hot-pressing process without any excessive post or pre-modification processes.

2. Experimental

2.1. Materials and chemicals

Commercial PAN polymer was purchased from the Isfahan Textile Co, Iran. Commercially available SAN polymer (SAN-4) was purchased from Ghaed Basir Co., Iran. DMSO, acetone, NaCl, and isopropyl alcohol (IPA) (extra-pure grade) were provided by Amertat Shimi, Co, Iran. Ctyltrimethylammoniumbromide (CTAB) and **sodium dodecyl sulfate (SDS) were** purchased from Merck, Germany. A commercial non-woven fabric made of polypropylene (PP) polymer was

used as support for nanofiber collection during the electroblowing process. Gasoline was provided by a local supplier.

2.2. Membrane fabrication process

The neat dual-layer PAN/SAN nanofibrous membrane was fabricated using PAN/DMSO + acetone (80 wt% DMSO and 20 wt% acetone; 8 wt% PAN) and SAN/DMSO + acetone (70 wt% DMSO and 30 wt% acetone; 17.5 wt% SAN) spinning solutions. Also, a small amount of CTAB salt was added to the spinning solution to reduce bead-on-string nanofibers. The electroblowing condition is summarized in Table 1. A co-axial electroblowing needle and syringe were attached via a polyethylene (PE) tube. With the help of a dry air flow, a continuous nanofiber jet was formed on the PP non-woven mat. First, a nanofibrous SAN layer was fabricated and then a nanofibrous PAN layer was fabricated on the support SAN layer. After completing the electroblowing process, the neat PAN/SAN nanofibrous membrane (designated as PAN/SAN) was immediately hot-pressed (H-PAN/SAN) under 2000 psi pressure at a temperature of 85 ℃ for 30 s to improve the physical integrity of the produced dual-layer nanofibrous membrane. A single-layer SAN nanofibrous membrane (designated as SAN) was also fabricated and hot-pressed (designated as H-SAN) to form a more uniform structure.

Table 1. Process parameters of the electroblowing process.

Nanofibrous layer	Voltage (kV)	Working distance (cm)	Polymer injection rate (µL/min)	Air flowrate (NL/min)	Spinning time (min)
PAN	22	30	90	2.5	45
SAN	18	30	90	2	45

2.3. Characterization

Surface morphology of the prepared nanofibrous layers and cross-sectional images of PAN/SAN nanofibrous membrane were observed by scanning electron microscopy (SEM, AIS 2100C, Korean Republic). The dual-layer H-PAN/SAN membrane was fractured in liquid nitrogen before the SEM test. Fiber diameter was measured by Digimizer software, and the average value of 100 fiber diameters was reported.

The thickness of the samples was measured using an accurate micrometer and cross-sectional images. The mean value of the three tests was reported as the mean thickness value.

The porosity was evaluated using the gravimetric method. First, membrane tickets were heated at 80 ℃ using a digital oven for 4 h to remove moisture and then weighed to determine the samples' dry weight. For the next step, pre-dried samples were submerged in IPA and reweighed. A full description of the process can be found in Zhou et al. [34].

The surface hydrophobicity of the prepared samples was determined by measurement of the water contact angle (WCA) using a drop shape analyzer device (KRUSS analyzer-G10 Drop Shape Analyzer, Germany). The underwater oleophobicity of the fabricated samples was measured by underwater oil contact angle (UOCA) using the same device.

The pore size of the single-layer SAN and dual-layer PAN/SAN membranes were measured using a lab-made bubble-point set-up. See Niknejad et al. [35] for more information.

The liquid entry pressure (LEP) of water was evaluated by a homemade set-up. Briefly, a circular-shaped sample of the dual-layer PAN/SAN and single-layer SAN membranes were placed between semi-cell modules. Pressure (kPa) was gradually increased to the point where the first deionized (DI) water droplet was observable on the membrane surface, and this pressure was regarded as the LEP value. The mean value of the three tests using independent membranes was reported.

2.4. DCMD process

A lab-scale DCMD set-up was used to evaluate the prepared membranes for saline and saline oily feeds. The representation of the DCMD device can be found in Bonyadi et al. [36]. The synthetic saline oily water was prepared by adding 1 g gasoline and 35 g NaCl to the DI water using a high-speed blender (rotating speed, 5000 rpm; mixing time, 1 h). Feed and permeate temperatures were 60 ± 1 ℃ and 25 ± 1 ℃, respectively. Feed and permeate streams were both set at 0.48 L/min. The feed water was mixed every 2 hours using the blender for about 5 minutes to ensure that the oil dispersion was uniform when it comes in contact with the active side of the membrane (hydrophilic layer). Also, the components of the DCMD set-up were mostly made from polyurethane (pipes) and polyethylene (feed tanks and membrane module). Therefore, the saline oily feed was circulated at least three times before starting the DCMD tests using a pump to ensure that the oil adhesion on the equipment was kept at a minimum during the DCMD tests to ensure a more accurate result. The mass and quality of the purified water were regularly monitored using a digital balance and an electrical conductivity (EC) meter, respectively. By knowing the active membrane surface area (m^2), the period of the recorded weight (h), and the amount of added water into the permeate tank (kg), the permeate flux (kg/m^2 h) could be determined.

3. Results and discussion

3.1. Morphology

The surface morphology of the top and bottom layers of the PAN/SAN membrane and the cross-sectional SEM image of the H-PAN/SAN membrane are shown in Fig 1. It is noteworthy that the morphology of the single-layer SAN was the same as the bottom layer of the PAN/SAN

membrane, as they were fabricated and hot-pressed under the same operating conditions. Therefore, only one SEM image is presented.

The polymer concentration in the dope solution is one of the deciding factors of the electrospinning process. For example, under the same electrospinning parameters, using dope solutions with low polymer concentrations will lead to the formation of cup-like defects and beaded fibers. However, raising the polymer concentration might result in a fiber diameter increase [37,38]. Therefore, the desirable morphology for the nanofibers can be obtained by controlling the polymer concentration. As observed, a defect-free nanofibrous SAN substrate with 3D microporous interconnected networks was fabricated with a suitable polymer concentration and CTAB addition to the dope solution [39]. For the PAN top layer, to maintain a balance between defects and fiber diameter enhancement, a microporous dense interconnected with minimal defects was fabricated by choosing the suitable polymer concentration.

For the dual-layer membrane, the mean fiber diameter of the neat SAN, hot-pressed SAN, neat PAN, and hot-pressed PAN was measured as 431 ± 58, 453 ± 32, 157 ± 48, and 174 ± 34 nm, respectively. Throughout the hot-pressing process, the mean fiber diameter was essentially constant because the temperature, pressure, and duration were not high enough to lead to an increase in fiber diameter while they were sufficient to increase fiber density by effectively compacting more nanofibers in a specific area [40]. Fig S1 Shows the cross-sectional SEM image for the H-PAN/SAN membrane after sonication to prove the robustness of the formed layer.

Visible changes in the pore size of the membranes can be observed after the hot-pressing process (Table 2). The hot-pressed samples had a smaller mean pore size compared to the neat membranes, which is evident by the naked eye. The cross-section image shows that the PAN and SAN layers are closely bonded with no signs of delamination at the PAN/SAN interface (Fig 1).

This can be attributed to the effective hot-pressing and the residual DMSO in the nanofibers, which further facilitate the adhesion at the PAN/SAN interface and reduces the probability of layer delamination.

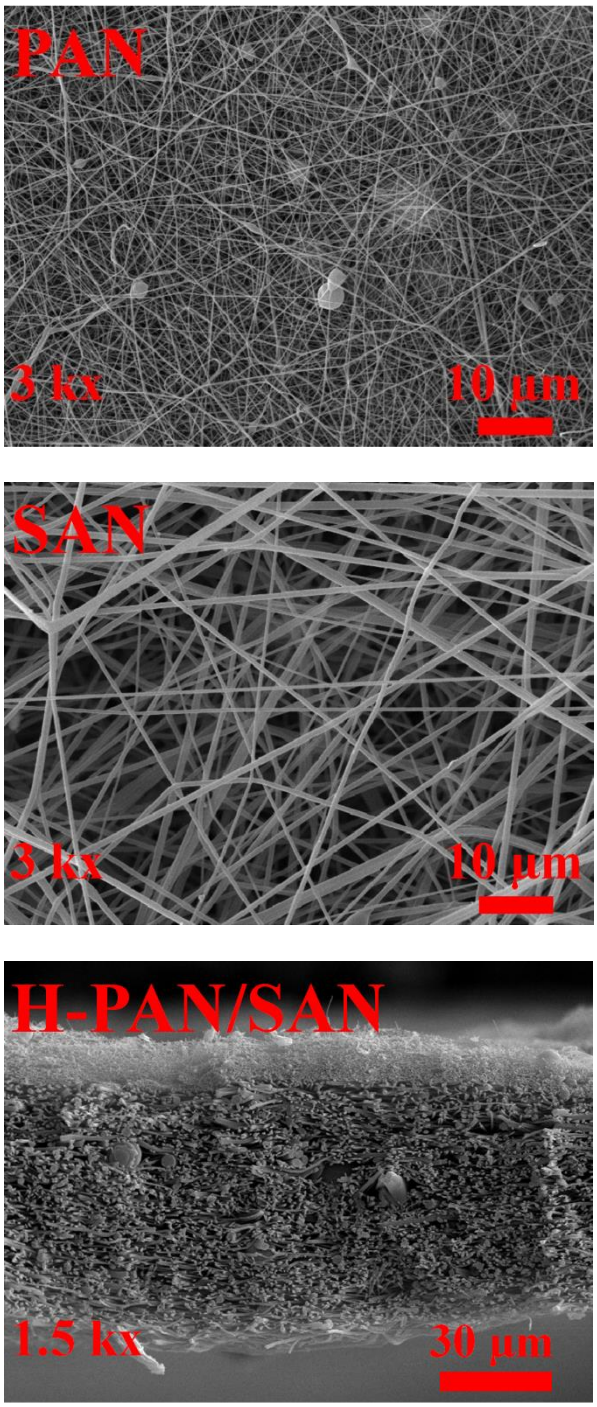

Fig 1. The surface morphology of the top layer, the bottom layer, and also the cross-section morphology of the fabricated PAN/SAN and H-PAN/SAN membranes. The SEM images' magnification with their scale bar is also presented.

3.2. Porosity and thickness

Electrospun nanofibrous membranes typically have higher porosities when compared to membranes fabricated via other membrane fabrication methods [35]. A membrane fabricated via the electroblowing process has a higher porosity than a membrane fabricated via the conventional electrospinning process (>95%). Moreover, using a longer spinning duration and a PP nonwoven mat while the charge density is kept constant can assist in making the fabricated membrane more porous by increasing the resistance against the electrical charge [41].

Higher porosity is favorable as permeability correlates positively with the porosity of the applied membrane in the MD process due to trapped air in the membrane pores that act as an insulator, thus reducing the heat loss by conduction and the water vapors having more space to pass through as a result of an increase in mean free path [35]. However, the downside is that these membranes have a larger pore size, loose and random fiber structure, wider pore size distribution, and insufficient mechanical strength that makes them inapplicable in the MD process [32]. After the hot-pressing process, the porosity of the membranes showed a declining trend. The porosity for neat SAN and PAN/SAN membranes dropped from 97.8 ± 2% and 95.7 ± 2% to 78.5 ± 1% and 75.4 ± 1%, respectively. This result is also in conformity with the declining trend reported by Yao et al. [42].

Table 2. Thickness, δ; porosity, ε; mean pore size, r_{mean}; maximum pore size, r_{max}; water contact angle, WCA; liquid entry pressure, LEP of the fabricated membranes.

Membrane	δ (µm)	ε (%)	r_{mean} (µm)	r_{max} (µm)	WCA (°)	UOCA (°)	LEP (kPa)
SAN	540 ± 50	97.8 ± 2	1.64 ± 0.03	4.12 ± 0.04	147.1 ± 1	76.2 ± 1	41.1 ± 2
H-SAN	64 ± 3	78.5 ± 1	0.43 ± 0.02	0.91 ± 0.02	142.3 ± 1	70.4 ± 1	120.3 ± 2
PAN/SAN	845 ± 50	95.7 ± 2	0.58 ± 0.02	1.32 ± 0.01	112.2 ± 1[a] 147.1 ± 1[b]	122.5 ± 1	65.3 ± 2
H-PAN/SAN	77 ± 3	75.4 ± 1	0.27 ± 0.01	0.52 ± 0.02	37.5 ± 1[a] 141.7 ± 1[b]	158.1 ± 1	156.2 ± 2

[a] top layer WCA
[b] bottom side WCA of SAN layer

Membrane thickness is another important parameter that affects the permeate flux, mechanical properties, and salinity the membrane can efficiently handle. The increase in salinity causes a drop in feed vapor pressure, consequently, if the transmembrane temperature is not high enough the loss in energy efficiency becomes considerable [43]. Although thicker membranes have higher energy efficiency, the driving force is insufficient to fully boost permeation. These membranes are preferable in the treatment of highly saline waters due to possible mass transfer resistance and a lower permeate flux [44,45]. Therefore, to achieve higher rejection and permeate flux, it is essential to determine a suitable balance between porosity and thickness. The thickness value for the neat SAN and PAN/SAN membranes reduced from 540 ± 50 and 845 ± 50 µm to 64 ± 3 and 77 ± 3 µm for the H-SAN and H-PAN/SAN, respectively. The porosity and thickness of the fabricated membranes show that the hot-pressed membranes have lower porosity and thickness values compared to the neat samples [42]. Thus, the permeability and rejection can be enhanced through a straightforward hot-pressing process [32].

3.3. Wettability

One of the major obstacles to the universality of MD is membrane wetting. The wetting phenomenon starts with the larger pores, and then gradually spreads throughout the whole membrane. Therefore, a larger maximum pore size is not favorable. While the pore size range applicable for MD membranes is between 0.1 and 1 µm, the preferred pore size for membranes applied for the MD process is reported to be in the range of 0.2 - 0.5 µm [12,46]. There are several factors to assess the wetting tendency of a membrane during the MD process such as WCA, maximum pore size, and LEP, which will be discussed later in this section. Moreover, the relationship of WCA, maximum pore size, and LEP is governed by the Laplace-Young equation ($LEP= -(\beta\gamma_1 \cos \theta)/r_{max}$) [47]. In simpler terms, to fabricate an optimal membrane, a balance between the abovementioned factors must be met. A membrane suitable for MD application should have a higher WCA, smaller maximum pore size, and a higher LEP value [48]. However, a hydrophobic membrane in the presence of oil in the saline feed is prone to pore blockage and pore wetting due to the hydrophobic-hydrophobic interaction between the oily content and the membrane surface. Therefore, the top layer that is in contact with the saline oily feed should be oleophobic enough to prevent pore blockage and wetting by forming a hydration layer at the membrane feed interface [20,49].

The WCA and UOCA values of the fabricated membranes are tabulated in Table 2 and related images are shown in Fig 2. Surface hydrophobicity can be manipulated by altering surface roughness using various methods [50,51]. It is worth stating that membranes fabricated via the electrospinning process (using hydrophobic polymers) have intrinsically higher WCA compared to membranes fabricated via other methods (i.e., NIPS). This can be ascribed to the non-woven nature of the fabricated membranes, which elevates surface roughness to form a re-entrant structure [52]. The WCA for the neat and H-SAN was measured as 147.1 ± 1° and 142.3 ± 1°,

respectively. Since the surface energy is constant, the reduction can be attributed to a decrease in surface roughness caused by the hot-pressing process [32,42]. Additionally, the WCA for the bottom layer of the PAN/SAN membrane was measured as 147.1 ± 1° and 141.7 ± 1° for neat and hot-pressed ones, respectively. It is essentially the same as the H-SAN membrane since they were fabricated and hot-pressed under the same parameters. The WCA for the top layer of the neat and hot-pressed PAN/SAN membranes was measured as 112.2 ± 1° and 37.5 ± 1°, respectively. This sharp decline can be ascribed to the highly rough surface of the neat PAN membrane that increases the amount of trapped air underneath the membrane. Moreover, the reported WCAs in Table 2 were measured immediately after placing a water droplet on the surface. Once the hot-pressing process was applied, surface roughness was reduced to considerably boost hydrophilicity. In addition, UOCA was improved from 122.5º for the PAN/SAN membrane to 158.1º for the H-PAN/SAN membrane. So, the oil repellency of the top layer underwent substantial enhancement by simply employing the hot-pressing process. A film showing the behavior of a gasoline droplet when contacting the top surface of the H-PAN/SAN is provided as supporting data (Video S1).

As mentioned previously, the existence of large pores may lead to partial pore wetting which will eventually lead to total wetting. Therefore, a hot-pressing process can significantly enhance the wetting resistance of the fabricated membrane. As seen in Table 2, the maximum pore size for the neat SAN and the neat PAN/SAN membrane decreased from 4.12 ± 0.04 and 1.32 ± 0.01 µm to 0.91 ± 0.02 and 0.52 ± 0.02 µm, respectively. The reported values are in the favorable range reported by Pan et al. [46]. The largest maximum pore size and mean pore size were measured for the neat SAN membrane, which results in a larger fiber diameter with a fluffy structure of the fabricated membrane. The smallest pore size was for the hot-pressed PAN/SAN membrane due to its compact structure.

The LEP value is the minimum transmembrane pressure exerted that will lead to the liquid feed overcoming the repellency of the hydrophobic surface and wetting the pores. [49] LEP value is one of the most important determining factors indicating the wetting resistance of the fabricated membranes because higher LEP values can guarantee a superior anti-wetting performance throughout the MD process. Table 2 demonstrates that higher LEP values have a better anti-wetting performance for the fabricated membranes. For the hot-pressed membranes compared to the corresponding neat membranes, the LEP value increased considerably. The LEP value for the neat SAN and neat PAN/SAN membranes increased from 41.1 ± 2 and 65.3 ± 2 kPa to 120.3 ± 2 and 156.2 ± 2 kPa for the H-SAN and H-PAN/SAN membrane, respectively. This can be attributed to a decline in the maximum pore size because they are inversely correlated according to the Laplace-Young equation [53,54].

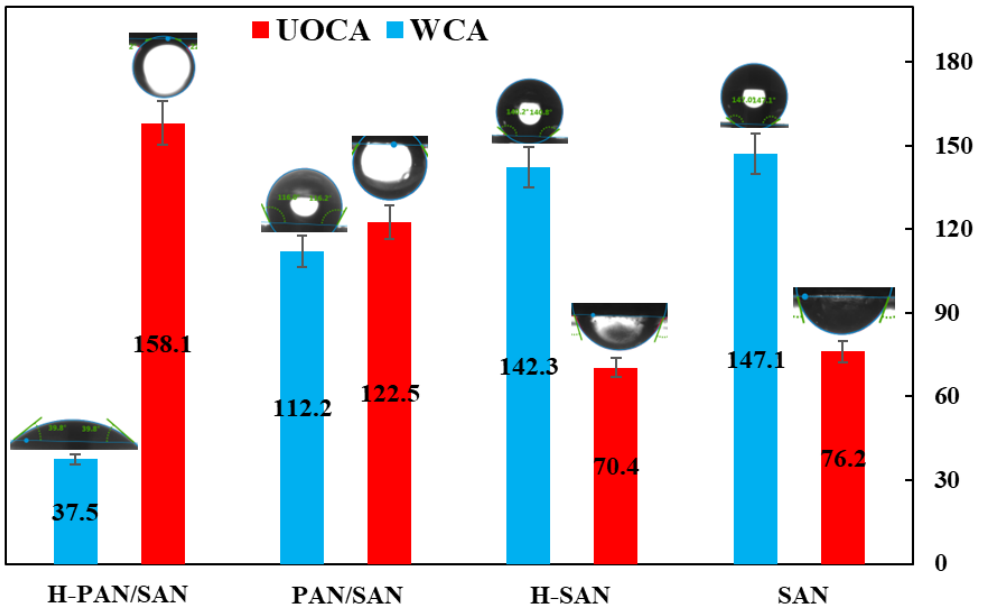

Fig 2. A diagram showing the in-air WCA and UOCA measurements for the used membranes in this study. The top layer of the membranes was used to measure these values. As an

example, in-air WCA for H-PAN/SAN was measured by placing DI water on the top of the membrane (PAN nanofibrous layer). To measure UOCA using the same membrane, it was immersed in water to contact the gasoline droplet to the top layer. Video S1 clearly shows how UOCA tests were performed.

3.4. DCMD

DCMD performance of the H-SAN and H-PAN/SAN membranes using saline water and oily saline water as a feed was thoroughly investigated. The neat membrane was not further assessed due to low mechanical strength (see ref. [52]), large maximum pore size (>1 µm, see Table 2), low LEP value, as well as high thickness [32]. It is a well-known fact that the existence of contaminants in the feed water can lead to partial wetting or pore blockage of the membrane, which will adversely affect MD performance [55,56]. Due to the composition of the saline oily feed, the wetting phenomena can be identified by observing the water conductivity in the permeate. The DCMD operating condition such as temperature difference (ΔT = 35 °C), feed concentration, and permeate flow rates (0.48 L/min) were kept constant during the 24 h test.

Fig 3 shows flux-time and conductivity-time profiles for the hot-pressed SAN and H-PAN/SAN membranes using saline water (Fig 3-A) and oily saline water (Fig 3-B) as a feed. Using the saline feed, a mean permeate flux of 42.26 and 34.89 kg/m^2 h was measured for the H-SAN and H-PAN/SAN, respectively. The H-SAN membrane achieved a higher flux compared to the dual-layer H-PAN/SAN membrane in saline water. The lower permeate flux for the H-PAN/SAN membrane can be attributed to the additional mass transfer resistance of the PAN top layer. The final EC value for the tested membranes did not exceed 5 µS/cm. The EC value showed no sign of membrane wetting in both cases since it does not demonstrate a rising trend. Also, both membranes

demonstrated high rejection (>99.9%) without a decline in permeate flux during the DCMD process due to high hydrophobicity and a proper LEP value.

Fig 3-B shows the DCMD performance of the membranes for treatment of the saline oily feed. In the presence of oil, the H-PAN/SAN membrane showed a high rejection (>99.9%), without a decline in permeate flux during the DCMD process, while in the case of the single-layer H-SAN membrane, the permeate flux sharply dropped due to pore blockage caused by the hydrophobic-hydrophobic interaction. Moreover, the adsorption of oil can increase the probability of pore wetting [57]. The membrane wetting is confirmed by the increase in EC value depicted in Fig 3-B. The mean permeate flux for the H-PAN/SAN membrane was 32.80 kg/m^2 h, which shows a 6% reduction in the permeate flux when compared to the saline water. This flux reduction can be caused by the formation of an oily layer that restricts the evaporation area [58]. The salt rejection of the H-PAN/SAN membrane also demonstrated the effect of a strong hydration layer between the membrane and oil droplets.

Fig 4 shows the DCMD performance of the H-PAN/SAN membrane for treating SDS-including saline oily feed (SDS concentration, 0.2 mM; salt concentration, 35 g/L; gasoline concentration, 1 g/L). Permeate flux and salt rejection were measured as 31.97 ± 2 kg/m^2 h and >99.9%, respectively, during 9 h continuous test. Applied DCMD conditions were the same as the previous tests (Temperature differences. 35 ℃; feed and permeate flow rates, 0.48 L/min). A negligible reduction in permeate flux was observed due to temporary fouling by smaller oil droplets. However, superior under water oil repellency of the H-PAN/SAN membrane by creating a strong hydration layer made a proper barrier for reversable fouling of oil droplets as these small oil particles can join together to form a bigger oil droplet to

detach easily for the surface. Also, small pore size of the nanofibrous PAN layer can help to repel oil droplets to keep DCMD process going.

A literature survey of recent work regarding dual-layer membranes is provided in Table 3. The tabulated works were used for saline oily water treatment using the DCMD process. The salt (35 g/L) and oil concentrations (1 g/L crude oil expect for this work) were the same when compared to the reported results. The H-PAN/SAN membrane was comparable with the literature considering UOCA. Due to the superior hydrophilicity of the PAN top layer in the dual-layer structure, a superoleophobic surface was observed. It can sufficiently repel oil droplets to keep the DCMD performance at a good level (i.e., high salt rejection without any change in flux). Considering environmental issues and cost-effectiveness, the proposed dual-layer membrane outperforms the other membranes by using a straightforward and eco-friendly hot-pressing, low-toxic DMSO solvent, productive electroblowing process, and low-priced membrane materials.

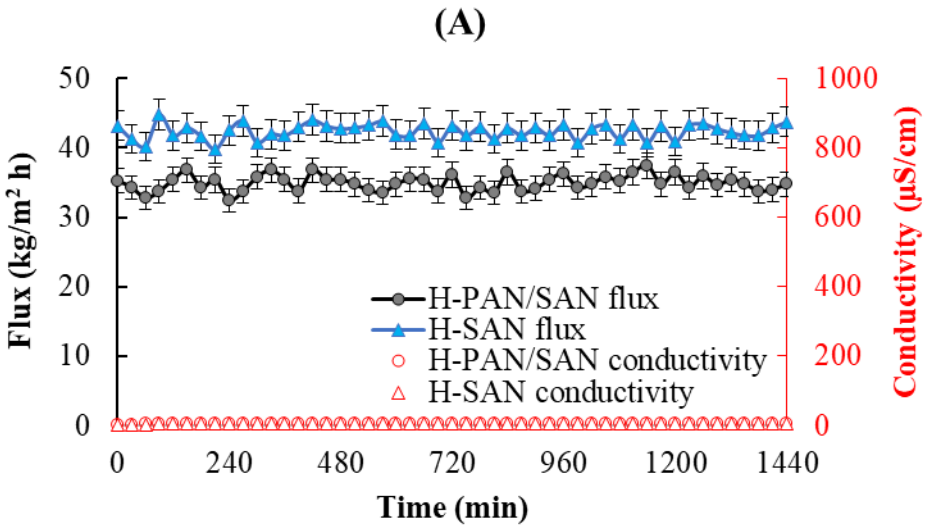

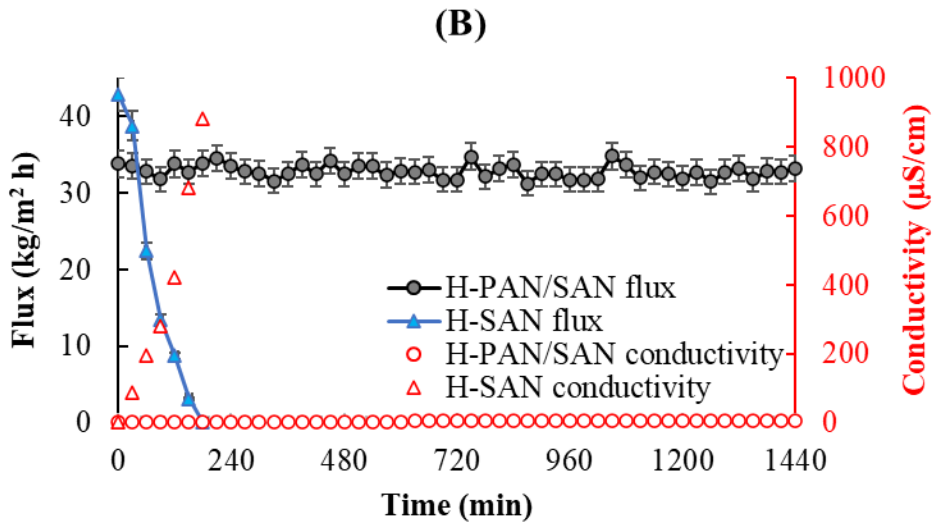

Fig 3. DCMD performance of the H-SAN and H-PAN/SAN using (A) saline water (35 g/L NaCl) and (B) oily saline water as feed. The temperature of feed and permeate were 60 ± 1 and 25 ± 1 ℃, respectively. Moreover, the flow rate of 0.48 L/min was applied to the feed and permeate sides.

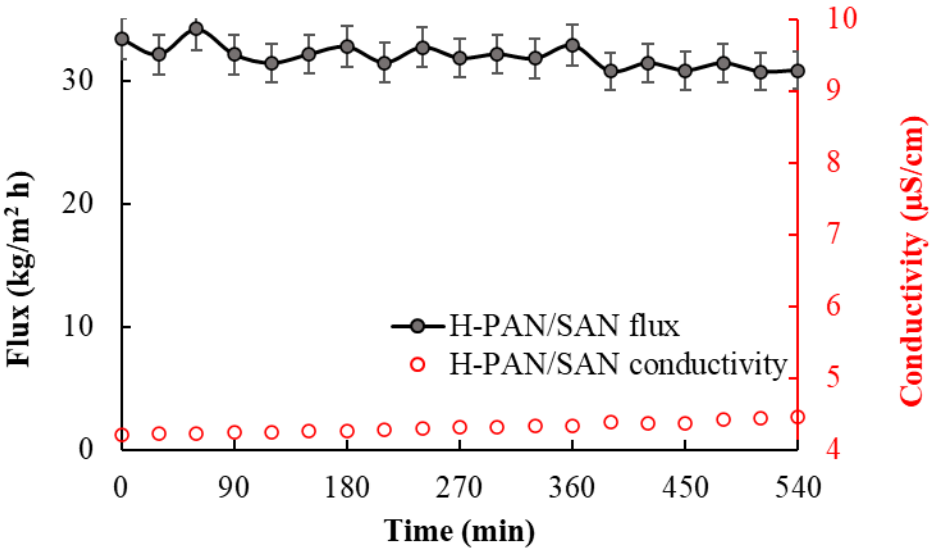

Fig 4. DCMD performance of H-PAN/SAN membrane for treating SDS-including saline oily water feed solution. Temperature difference and feed/permeate flow rate were set at 35 ℃ and 0.48 mL/min, respectively.

Table 3. Physical characteristics and DCMD performance of recently published flat-sheet membranes for saline oily treatment (35 g NaCl + 1 g oil/L).

Membrane	UOCA (°)	ε (%)	r_{mean} (µm)	δ (µm)	LEP (kPa)	Flux (kg/m^2 h)	ΔT (°C)	t_{DCMD} (h)	R (%)	Reference
Janus NFMs	164	-	1.45	66	136.0	25.4	40	30	100	[29]
Modified PVDF	149.5	72.5	0.38	180.1	326	26.1	40	36	100	[18]
PTFE/PAN-OH	161.7	69.8	0.21	267.8	375	15.2	33	25	~100	[59]
CTS/PFO-PVDF	>130	-	-	177.5	300	27.0	40	36	99.9	[60]
PTFE/PVA-Si-GA	156.5	41.6	0.41	348.0	-	17.5	33	50	100	[20]
PTFE/CA-SiNPs	154.2	50.6	0.47	303.0	-	~19.9 [a]	33	30	-	[28]
PTFE-9CA	158	62.5	0.21	248	371	16.85	33	18	100	[61]
H-PAN/SAN	158.1	75.4	0.27	77	156.2	32.80	35	24	>99.9	Current work

[a] Initial flux

4. Conclusion

For the treatment of saline oily water by DCMD, an eco-friendly and inexpensive PAN/SAN membrane was fabricated. In order to boost the production rate, the electroblowing process was implemented using a low-toxic DMSO solvent to fabricate a dual-layer PAN/SAN membrane. Then, through a simple hot-pressing process, the membrane characteristics including a decrease in surface hydrophobicity and an increase in the LEP value were manipulated in a way to meet the demands of the MD process. Interaction between oil and the hydrophobic surface was mitigated by a layer of PAN nanofibers. As the PAN layer of the hot-pressed PAN/SAN membrane became underwater superoleophobic, nearly complete salt rejection without any considerable increase in EC value was measured while for the hot-pressed single-layer SAN membrane, the wetting started from the beginning of the DCMD process. It is hopeful that the anti-wetting and anti-fouling properties of the fabricated membrane can address the challenging issue of saline oily water treatment in a more scalable, eco-friendly, and cost-efficient manner.

Declaration of competing interest

The authors declare that they have no known competing financial interests or personal relationships that could have appeared to influence the work reported in this paper.

Acknowledgment

This work is dedicated to my father (Bahram Sallakh Niknejad) who backed me a lot during the past years. He is the sole provider of my published papers (11 papers) and I enjoy having him on my side.

Appendix A. Supplementary data

Cross-sectional morphology of sonicated H-PAN/SAN membrane is also provided in Fig S1. A video showing the nonstick character of the H-PAN/SAN membrane against gasoline was also provided in video S1.

References

[1] V. Karanikola, C. Boo, J. Rolf, M. Elimelech, Engineered slippery surface to mitigate gypsum scaling in membrane distillation for treatment of hypersaline industrial wastewaters, Environ. Sci. Technol. 52 (2018) 14362–14370.

[2] Y. Xu, J. Ma, D. Liu, H. Xu, F. Cui, W. Wang, Origami system for efficient solar driven distillation in emergency water supply, Chem. Eng. J. 356 (2019) 869–876.

[3] M.C. Tomei, V. Stazi, D.M. Angelucci, Biological treatment of hypersaline wastewater in a continuous two-phase partitioning bioreactor: analysis of the response to step, ramp and impulse loadings and applicability evaluation, J. Clean. Prod. 191 (2018) 67–77.

[4] B. Alkotaini, S.L. Tinucci, S.J. Robertson, K. Hasan, S.D. Minteer, M. Grattieri, Alginate-encapsulated bacteria for the treatment of hypersaline solutions in microbial fuel cells, Chembiochem 19 (2018) 1162–1169.

[5] S.F. Corsino, M. Capodici, M. Torregrossa, G. Viviani, Physical properties and extracellular polymeric substances pattern of aerobic granular sludge treating hypersaline wastewater, Bioresour. Technol. 229 (2017) 152–159.

[6] R. Zhang, J. Tian, S. Gao, B. Van der Bruggen, How to coordinate the trade-off between water permeability and salt rejection in nanofiltration? J. Mater. Chem. A 8 (2020) 8831–8847.

435 [7] G. Zuo, R. Wang, Novel membrane surface modification to enhance anti-oil fouling property
436 for membrane distillation application. J. Membr. Sci. 447 (2013) 26-35.

437 [8] L.D. Tijing, Y.C. Woo, J.S. Choi, S. Lee, S.H. Kim, H.K. Shon, Fouling and its control in
438 membrane distillation - A review. J. Membr. Sci. 475 (2015) 215-44.

439 [9] M.S. El-Bourawi, Z. Ding, R. Ma, M. Khayet, A framework for better understanding membrane
440 distillation separation process, J. Membr. Sci. 285 (2006) 4–29.

441 [10] A.K. An, J. Guo, S. Jeong, E.J. Lee, S.A.A. Tabatabai, T. Leiknes, High flux and antifouling
442 properties of negatively charged membrane for dyeing wastewater treatment by membrane
443 distillation, Water Res. 103 (2016) 362–371.

444 [11] C. Su, T. Horseman, H. Cao, K. Christie, Y. Li, S. Lin, Robust superhydrophobic membrane
445 for membrane distillation with excellent scaling resistance, Environ. Sci. Technol. 53
446 (2019) 11801–11809.

447 [12] A. Alkhudhiri, N. Darwish, N. Hilal, Membrane distillation: a comprehensive review,
448 Desalination 287 (2012) 2–18.

449 [13] Z. Xiao, R. Zheng, Y. Liu, H. He, X. Yuan, Y. Ji, D. Li, H. Yin, Y. Zhang, X.M. Li, T. He,
450 Slippery for scaling resistance in membrane distillation: a novel porous micropillared
451 superhydrophobic surface, Water Res. 155 (2019) 152–161.

452 [14] J.R. Werber, C.O. Osuji, M. Elimelech, Materials for next-generation desalination and water
453 purification membranes, Nat. Rev. Mater. 1 (2016) 16018.

[15] D.M. Warsinger, J. Swaminathan, E. Guillen-Burrieza, H.A. Arafat, H.L.V. John, Scaling and fouling in membrane distillation for desalination applications: a review, Desalination 356 (2015) 294–313.

[16] M. Rezaei, D.M. Warsinger, V.J. Lienhard, M.C. Duke, T. Matsuura, W.M. Samhaber, Wetting phenomena in membrane distillation: mechanisms, reversal, and prevention, Water Res. 139 (2018) 329–352.

[17] Z. Wang, S. Lin, Membrane fouling and wetting in membrane distillation and their mitigation by novel membranes with special wettability, Water Res. 112 (2017) 38–47.

[18] Z. Wang, D. Hou, S. Lin, Composite membrane with underwater-oleophobic surface for anti-oil-fouling membrane distillation, Environ. Sci. Technol. 50 (2016) 3866–3874.

[19] K.R. Zodrow, E. Barzeev, M.J. Giannetto, M. Elimelech, Biofouling and microbial communities in membrane distillation and reverse osmosis, Environ. Sci. Technol. 48 (2014) 13155–13164.

[20] D. Hou, C. Ding, K. Li, D. Lin, D. Wang, J. Wang, A novel dual-layer composite membrane with underwater-superoleophobic/hydrophobic asymmetric wettability for robust oil-fouling resistance in membrane distillation desalination, Desalination 428 (2018a) 240–249.

[21] X. An, Z. Liu, Y. Hu, Amphiphobic surface modification of electrospun nanofibrous membranes for anti-wetting performance in membrane distillation, Desalination 432 (2018) 23–31.

[22] J. Lee, C. Boo, W.H. Ryu, A.D. Taylor, M. Elimelech, Development of omniphobic desalination membranes using a charged electrospun nanofiber scaffold, ACS Appl. Mater. Interfaces 8 (2016) 11154–11161.

[23] Z. Zhu, Y. Liu, H. Hou, W. Shi, F. Qu, F. Cui, W. Wang, Dual-bioinspired design for constructing membranes with superhydrophobicity for direct contact membrane distillation, Environ. Sci. Technol. 52 (2018) 3027–3036.

[24] Y.X. Huang, Z. Wang, J. Jin, S. Lin, Novel Janus membrane for membrane distillation with simultaneous fouling and wetting resistance, Environ. Sci. Technol. 51 (2017) 13304–13310.

[25] L. Deng, P. Li, K. Liu, X. Wang, B.S. Hsiao, Robust superhydrophobic dual layer nanofibrous composite membranes with a hierarchically structured amorphous polypropylene skin for membrane distillation, J. Mater. Chem. A 7 (2019)11282–11297.

[26] S. Cong, F. Guo, Janus nanofibrous membranes for desalination by air gap membrane distillation, ACS Appl. Polym. Mater. 1 (2019) 3443–3451.

[27] K. Wang, D. Hou, J. Wang, Z. Wang, B. Tian, P. Liang, Hydrophilic surface coating on hydrophobic PTFE membrane for robust anti-oil-fouling membrane distillation, Appl. Surf. Sci. 450 (2018) 57–65.

[28] D. Hou, Z. Wang, K. Wang, J. Wang, S. Lin, Composite membrane with electrospun multiscale-textured surface for robust oil-fouling resistance in membrane distillation, Journal of Membrane Science, 546 (2018b) 179–187.

494 [29] Z. Zhu, Z. Liu, L. Zhong, C. Song, W. Shi, F. Cui, W. Wang, Breathable and asymmetrically
495 superwettable Janus membrane with robust oil-fouling resistance for durable membrane
496 distillation, J. Membr. Sci. 563 (2018) 602–609.

497 [30] M. Lou, X. Fang, Y. Liu, G. Chen, J. Zhou, C. Ma, H. Wang, J. Wu, Z. Wang, F. Li, Robust
498 dual-layer Janus membranes with the incorporation of polyphenol/Fe3+ complex for
499 enhanced anti-oil fouling performance in membrane distillation, Desalination 515 (2021)
500 115184.

501 [31] Z. Zhu, L. Zhong, X. Chen, W. Zheng, J. Zuo, G. Zeng, W. Wang, Monolithic and self-
502 roughened Janus fibrous membrane with superhydrophilic/omniphobic surface for robust
503 antifouling and antiwetting membrane distillation, J. Membr. Sci. 615 (2020) 118499.

504 [32] R. Sallakhniknezhad, M. Khorsi, A.S. Niknejad, S. Bazgir, A. Kargari, M. Sazegar, M.
505 Rasouli, S. Chae, Enhancement of Physical Characteristics of Styrene–Acrylonitrile
506 Nanofiber Membranes Using Various Post-Treatments for Membrane Distillation,
507 Membranes 11 (2021) 969.

508 [33] A.S. Niknejad, S. Bazgir, A. Kargari, Mechanically improved superhydrophobic nanofibrous
509 polystyrene/high- impact polystyrene membranes for promising membrane distillation
510 application, J. Appl. Polym. Sci. 138 (2021a) 50917.

511 [34] T. Zhou, Y. Yao, R. Xiang, Y. Wu, Formation and characterization of polytetrafluoroethylene
512 nanofiber membranes for vacuum membrane distillation, J. Membr. Sci. 453 (2014) 402–
513 408.

514 [35] A.S. Niknejad, S. Bazgir, A. Sadeghzadeh, M.M.A. Shirazi, Evaluation of a novel and highly
515 hydrophobic acrylonitrile-butadiene-styrene membrane for direct contact membrane

distillation: electroblowing/air-assisted electrospraying techniques, Desalination 500 (2021b) 114893.

[36] E. Bonyadi, A.S. Niknejad, F.Z. Ashtiani, S. Bazgir, A. Kargari, A well-designed polystyrene/polycarbonate membrane for highly saline water desalination using DCMD process, Desalination 528 (2022) 115604.

[37] B. Veleirinho, M.F. Rei, J.A. Lopes-DA-Silva, Solvent and concentration effects on the properties of electrospun poly(ethylene terephthalate) nanofiber mats, J. Polym. Sci. B: Polym. Phys. 46 (2008) 460–471.

[38] B. Tarus, N. Fadel, A. Al-Oufy, and M. El-Messiry, Effect of polymer concentration on the morphology and mechanical characteristics of electrospun cellulose acetate and poly (vinyl chloride) nanofiber mats, Alexandria Eng. J. 55 (2016) 2975–2984.

[39] L. Huang, S.S. Manickam, J.R. McCutcheon, Increasing strength of electrospun nanofiber membranes for water filtration using solvent vapor, J. Membr. Sci. 436 (2013) 213-220.

[40] H. Ke, M. Feldman, P. Guzman, J. Cole, Q. Wei, B. Chu, A. Alkhudhiri, R. Alrasheed, B.S. Hsiao, Electrospun polystyrene nanofibrous membranes for direct contact membrane distillation, J. Membr. Sci. 515 (2016) 86-97.

[41] A.S. Niknejad, S. Bazgir, A. Kargari, Novel Triple-Layer HIPS/SBR/PP Nanofibrous Membranes for Robust DCMD Desalination, Ind. Eng. Chem. Res 60 (2021c) 2911–2920.

[42] M. Yao, Y.C. Woo, L.D. Tijing, W.G. Shim, J.S. Choi, S.H. Kim, H.K. Shon, Effect of heat-press conditions on electrospun membranes for desalination by direct contact membrane distillation, Desalination 378 (2016) 80–91.

[43] L. Eykens, I. Hitsov, K. De Sitter, C. Dotremont, L. Pinoy, I. Nopens, B. Van der Bruggen, Influence of membrane thickness and process conditions on direct contact membrane distillation at different salinities, J. Membr. Sci. 498 vol. 498 (2016) 353-364.

[44] L. Eykens, K. De Sitter, C. Dotremont, W. De Schepper, L. Pinoy, B. Van Der Bruggen, Wetting Resistance of Commercial Membrane Distillation Membranes in Waste Streams Containing Surfactants and Oil, Appl. Sci. 7 (2017) 118.

[45] A.S. Niknejad, S. Bazgir, A. Sadeghzadeh, M.M.A. Shirazi, Styrene-acrylonitrile (SAN) nanofibrous membranes with unique properties for desalination by direct contact membrane distillation (DCMD) process, Desalination 488 (2020) 114502.

[46] C.-Y. Pan, G.-R. Xu, K. Xu, H.-L. Zhao, Y.-Q. Wu, H.-C. Su, J.-M. Xu, R. Das, Electrospun nanofibrous membranes in membrane distillation: Recent developments and future perspectives, Sep. Purif. Technol. 221 (2019) 44–63.

[47] O. Makanjuola, F. Ahmed, I. Janajreh, R. Hashaikeh, Development of a dual-layered PVDF-HFP/cellulose membrane with dual wettability for desalination of oily wastewater, J. Membr. Sci. 570–571 (2019) 418–426.

[48] N.G.P. Chew, S. Zhao, R. Wang, Recent advances in membrane development for treating surfactant- and oil-containing feed streams via membrane distillation, Adv. Colloid Interface Sci. 273 (2019) 102022.

[49] H. Chamani, J. Woloszyn, T. Matsuura, D. Rana, C.Q. Lan, Pore wetting in membrane distillation: A comprehensive review, Prog. Mater. Sci. 122 (2021) 100843.

[50] E. Celia, T. Darmanin, E. Taffin de Givenchy, S. Amigoni, F. Guittard, Recent advances in designing superhydrophobic surfaces, J. Colloid Interface Sci. 402 (2013) 1–18.

[51] M.K. Sarkar, K. Bal, F. He, J. Fan, Design of an outstanding super-hydrophobic surface by electro-spinning, Appl. Surf. Sci. 257 (2011) 7003–7009.

[52] A.S. Niknejad, S. Bazgir, A. Kargari, M. Barani, E. Ranjbari, and M. Rasouli, A high-flux polystyrene-reinforced styrene-acrylonitrile/polyacrylonitrile nanofibrous membrane for desalination using direct contact membrane distillation, J. Membr. Sci. 638 (2021d) 119744.

[53] G. Rácz, S. Kerker, Z. Kovács, G. Vatai, M. Ebrahimi, P. Czermak, Theoretical and experimental approaches of liquid entry pressure determination in membrane distillation processes, Periodica Polytech., Chem. Eng. 58 (2014) 81–91,

[54] Y. Liao, C.H. Loh, R. Wang, A.G. Fane, Electrospun superhydrophobic membrane with unique structure for membrane distillation, ACS Appl. Mater. Interfaces 6 (2014) 16035–16048,

[55] K.J. Lu, Y. Chen, T.-S. Chung, Design of omniphobic interfaces for membrane distillation—A review, Water Res. 162 (2019) 64–77.

[56] X. Du, Z. Zhang, K.H. Carlson, J. Lee, T. Tong, Membrane fouling and reusability in membrane distillation of shale oil and gas produced water: Effects of membrane surface wettability, J. Membr. Sci. 567 (2018) 199–208.

[57] M. Gryta, Resistance of Polypropylene Membrane to Oil Fouling during Membrane Distillation, Membranes 11 (2021) 552.

[58] L. Han, Y.Z. Tan, T. Netke, A.G. Fane, J.W. Chew, Understanding oily wastewater treatment via membrane distillation. J. Membr. Sci. 539 (2017) 284–294.

[59] M. Tang, D. Hou, C. Ding, K. Wang, D. Wang, J. Wang, Anti-oil-fouling hydrophobic-superoleophobic composite membranes for robust membrane distillation performance, Sci. Total Environ. 696 (2019) 133883.

[60] Z. Wang, S. Lin, The impact of low-surface-energy functional groups on oil fouling resistance in membrane distillation, J. Membr. Sci. 527 (2017) 68–77.

[61] M. Tang, K.S.S. Christie, D. Hou, C. Ding, X. Jia, J. Wang, Fabrication of a novel underwater-superoleophobic/hydrophobic composite membrane for robust anti-oil-fouling membrane distillation by the facile breath figures templating method, J. Membr. Sci. 617 (2021) 118666.

Manuscript Number: DES-D-23-00351R1

A scalable dual-layer PAN/SAN nanofibrous membrane for treatment of saline oily water using membrane distillation

Dear Prof. Tong,

Guest Editor of VSI: MD & MCr,

We would like to thank you and the respected reviewers. Revised sections were shown using the bold red color font for the readers to notice. A DCMD test with surfactant-including feed water was added to the manuscript.

Kind regards,

Ali Sallakh Niknejad (Email: *aliniknejad1991@gmail.com*)

Department of Chemical and Environmental Engineering, University of Cincinnati, Cincinnati, OH, USA

Ali Kargari (E-mail: *kargari@aut.ac.ir*)

Membrane Processes Research Laboratory (MPRL), Department of Chemical Engineering, Amirkabir University of Technology (Tehran Polytechnic), Tehran, Iran

Reviewer#3

1. The authors have not addressed the use of the surfactant containing feed. Unfortunately, the first author having moved to another institute does not seem to be a sufficient reason not to address this point.

Response: Revised sections are in bold red color font. Please refer to the following to see the revised sections below:

"Fig 4 shows the DCMD performance of the H-PAN/SAN membrane for treating SDS-including saline oily feed (SDS concentration, 0.2 mM; salt concentration, 35 g/L; gasoline concentration, 1 g/L). Permeate flux and salt rejection were measured as 31.97 ± 2 kg/m^2 h and >99.9%, respectively, during 9 h continuous test. Applied DCMD conditions were the same as the previous tests (Temperature differences. 35 ℃; feed and permeate flow rates, 0.48 L/min). A negligible reduction in permeate flux was observed due to temporary fouling by smaller oil droplets. However, superior under water oil repellency of the H-PAN/SAN membrane by creating a strong hydration layer made a proper barrier for reversable fouling of oil droplets as these small oil particles can join together to form a bigger oil droplet to detach easily for the surface. Also, small pore size of the nanofibrous PAN layer can help to repel oil droplets to keep DCMD process going.

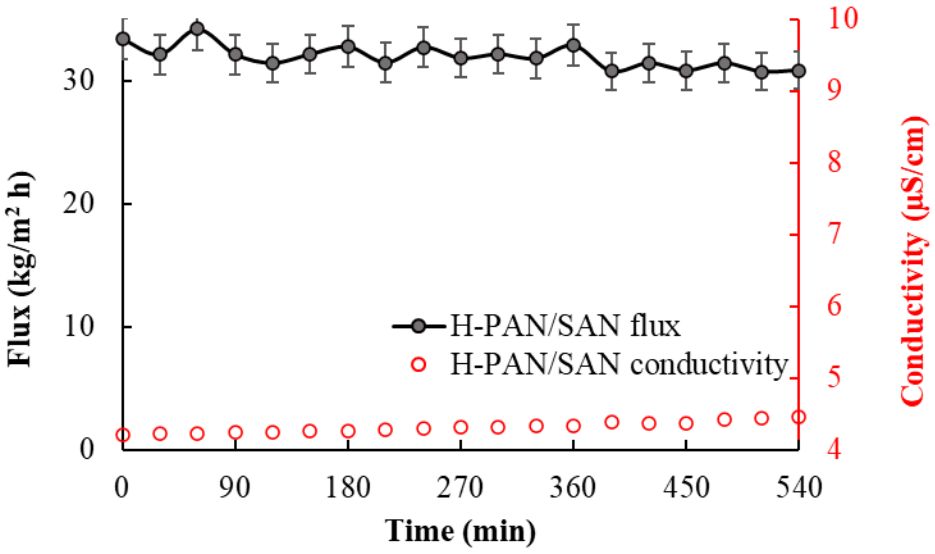

Fig 4. DCMD performance of H-PAN/SAN membrane for treating SDS-including saline oily water feed solution. Temperature difference and feed/permeate flow rate were set at 35 ℃ and 0.48 mL/min, respectively. “

2. If the authors' main novelty is hot pressing, they need to show what the hot press does physically and chemically, with sufficient characterization and impact of pressing conditions. Simply showing that hot press improves hydrophilicity does not seem to be sufficient to support the claimed novelty.

Response: The pressing process concept to improve the physical characteristics of the nanofibrous structures is well established in the literature. As the hot-pressing temperature is well below the melting and glass transition temperatures of the used polymers, chemical investigation is not necessary as we used these membranes without *any chemical modification*. Hot-pressing process gives more uniform physical characteristics like reduced pore size and thickness, improved mechanical strength as well as reduced hydrophobicity because of roughness reduction. It needs to be stated that polyacrylonitrile (PAN) is a hydrophilic polymer and water contact angle (WCA) of the neat fibrous structure depends on different factors during the membrane fabrication process. Air/gas-assisted electrospinning or electroblowing can make nanofibrous membrane surface even more rough, since we used non-conductive PP non-woven layer as support to collect nanofibers instead of aluminum foil. The spinning speed of the electroblowing is so much higher than regular electrospinning process making nanofibrous layer least organized to increase surface roughness as air flow adds another turbulency to the fibers’ journey toward the collector. Nanofibrous membrane is getting thicker and thicker by passing of time due to increasing fiber repulsion as evident in Table 2. Also, polarity of the polymer is another factor to have either a uniform or less organized fibrous layer. Based on our experience, an electroblown PVDF nanofiber membrane is more compact, and porosity of the neat fibrous structure is lower than 94% showing the effect of polymer polarity on the characteristics of final product. As a result, above mentioned factors led to a higher porosity (> 97%) for electroblown nanofibrous membranes compared to that of electrospun nanofibers. Based on the literature review we did, a wide range of WCA was reported for *neat* electrospun PAN nanofibers from 118.2 [1] down to 66.1° [2]. So, surface roughness is the main

reason for these variations in WCA, and after hot-pressing process the surface becomes uniform to reduce WCA. In our previous work conducted by Sadeghzadeh et al. [3], nanofibrous polystyrene (PS) membranes were fabricated using the same electroblowing device we used in this study and the mean surface roughness was reduced from 428 to 290 nm after hot-pressing. Also, Shirazi et al. [4] used the same device to form electrospun PS nanofibers and they reported mean roughness of 301 nm showing that electroblowing forms a surface with more roughness. We mentioned these factors inside the manuscript to explain why WCA reduced sharply.

As we mentioned in the first revision stage, it is the first report to use pressing process to design a **Janus nanofibrous membrane** for **saline oily water treatment** with **no chemical modification**.

[1] Zhang, L., He, Y., Ma, L., Chen, J., Fan, Y., Zhang, S., Shi, H., Li, Z. and Luo, P., 2019. Hierarchically stabilized PAN/β-FeOOH nanofibrous membrane for efficient water purification with excellent antifouling performance and robust solvent resistance. ACS applied materials & interfaces, 11(37), pp.34487-34496.

[2] Yalcinkaya, F., Yalcinkaya, B., Pazourek, A., Mullerova, J., Stuchlik, M. and Maryska, J., 2016. Surface modification of electrospun PVDF/PAN nanofibrous layers by low vacuum plasma treatment. International Journal of Polymer Science, 2016.

[3] Sadeghzadeh, A., Bazgir, S., & Shirazi, M. M. A. (2020). Fabrication and characterization of a novel hydrophobic polystyrene membrane using electroblowing technique for desalination by direct contact membrane distillation. Separation and Purification Technology, 239, 116498.

[4] Shirazi, M. M. A., Kargari, A., Bazgir, S., Tabatabaei, M., Shirazi, M. J. A., Abdullah, M. S., ... & Ismail, A. F. (2013). Characterization of electrospun polystyrene membrane for treatment of biodiesel's water-washing effluent using atomic force microscopy. Desalination, 329, 1-8.

Highlights

- ✓ Nanofibrous PAN/SAN membrane fabrication using electroblowing process.
- ✓ Fast hot-pressing process to form underwater superoleophobic membrane.
- ✓ UOCA of ~158° and in-air WCA of ~37° because of hot-pressing.
- ✓ Robust DCMD performance using saline oily water as feed.

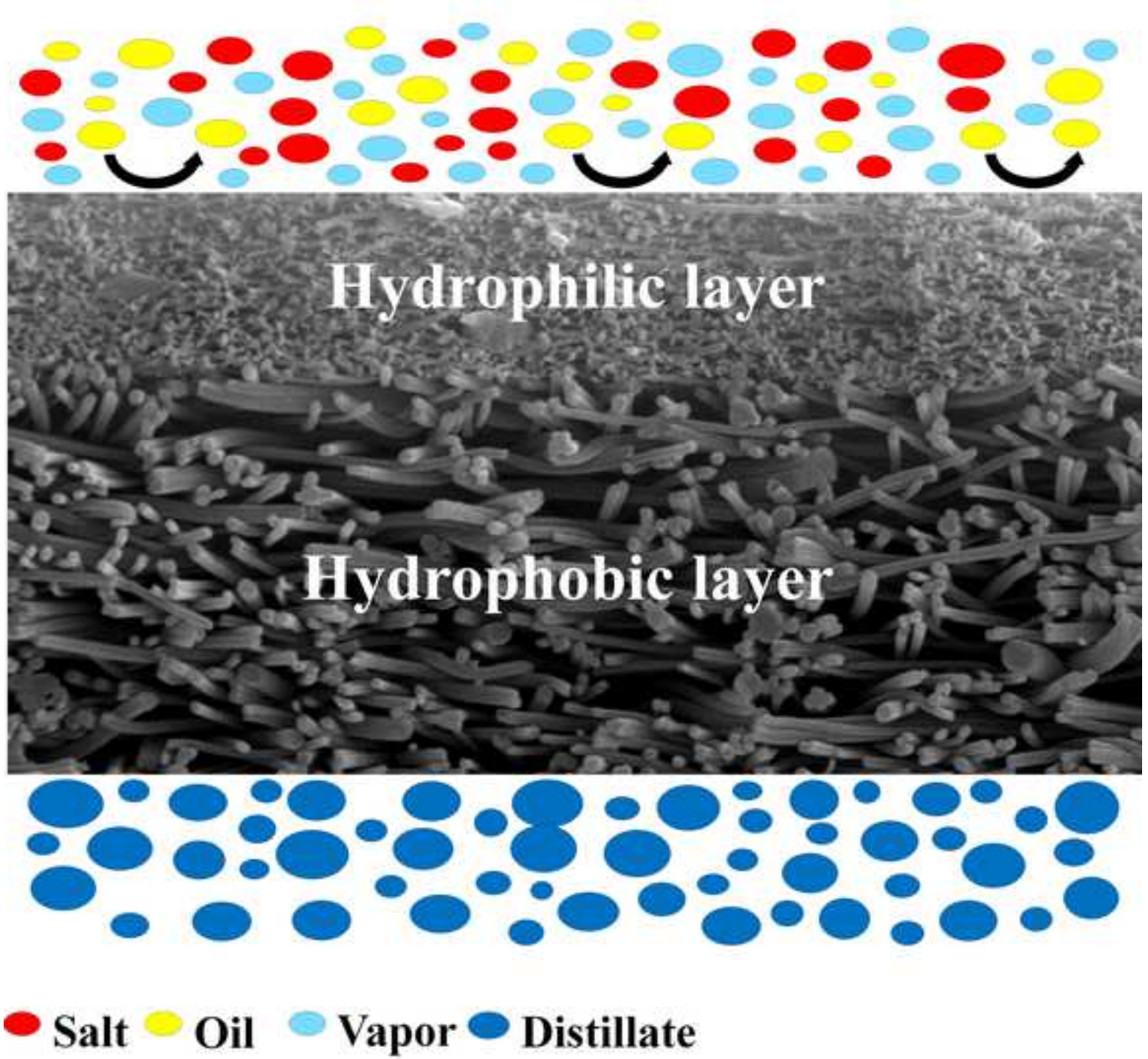

Declaration of interests

☒The authors declare that they have no known competing financial interests or personal relationships that could have appeared to influence the work reported in this paper.

☐The authors declare the following financial interests/personal relationships which may be considered as potential competing interests:

CRediT authorship contribution statement

Ali Sallakh Niknejad: Investigation, Writing - Original Draft, Writing - Review and Editing Conceptualization, Visualization, Supervision. **Ali Kargari:** Writing - Review and Editing, Validation, Supervision. **Mahsa Namdari:** Writing - Review and Editing. **Mohammad Pishnamazi:** Writing - Review and Editing. **Reza Sallakhniknezhad:** Writing - Original Draft. **Masoud Barani:** Resources. **Esmaeil Ranjbari:** Resources. **Saeed Bazgir:** Resources. **Mohsen Rasouli:** Resources. **Drew McAvoy:** Writing - Review and Editing.

A scalable dual-layer PAN/SAN nanofibrous membrane for treatment of saline oily water using membrane distillation

Ali Sallakh Niknejad [*1,4], Ali Kargari [*2], Mahsa Namdari [3], Mohammad Pishnamazi [1], Masoud Barani [4], Esmaeil Ranjbari [4], Reza Sallakhniknezhad [5], Saeed Bazgir [4,6], Mohsen Rasouli [7], Drew McAvoy [1]

[1] *Department of Chemical and Environmental Engineering, University of Cincinnati, Cincinnati, Ohio, USA*

[2] *Membrane Processes Research Laboratory (MPRL), Department of Chemical Engineering, Amirkabir University of Technology (Tehran Polytechnic), Tehran, Iran*

[3] *Department of Chemical Engineering, Amirkabir University of Technology, Tehran, Iran*

[4] *Nano polymer Research Laboratory (NPRL), Science and Research Branch, Islamic Azad University, Tehran, Iran*

[5] *School of Mechanical Engineering, Beijing Institute of Technology, Beijing, China*

[6] *Department of Polymer Engineering, Petroleum and Chemical Engineering Faculty, Science and Research Branch, Islamic Azad University, Tehran, Iran*

[7] *SEM Lab, Central Laboratory, Amirkabir University of Technology, Tehran, Iran*

Corresponding authors:

Ali Sallakh Niknejad (Email: *aliniknejad1991@gmail.com*; *sallakai@mail.uc.edu*)

Ali Kargari (Tel/fax: +98-21-66405847; E-mail: *kargari@aut.ac.ir*; *ali_kargari@yahoo.com*)

Abstract

Single-layer hydrophobic membranes are prone to fouling while subjected to a feed containing hydrophobic contaminants. In this study, using the green solvent Dimethyl sulfoxide (DMSO), dual-layer nanofibrous poly-acrylonitrile (PAN)/styrene-acrylonitrile (SAN) membranes were fabricated using the highly productive electroblowing process. Then through a simple hot-pressing process, the desirable hydrophilicity was achieved for PAN/SAN membrane. The water contact angle (WCA) for the top layer fell from 112.2 ± 1° to 37.5 ± 1° after hot-pressing, while the WCA for the bottom layer decreased slightly from 147.1 ± 1° to 142.3 ± 1°. Moreover, an underwater oil contact angle (UOCA) of 158.1 ± 1° was achieved for the PAN/SAN membrane. Direct contact membrane distillation (DCMD) tests were performed for synthetic saline water and synthetic saline oily water. While the permeate flux dropped for the single-layer SAN membrane, the dual-layer PAN/SAN membrane, due to underwater superoleophobicity, achieved a stable permeate flux for 24 h with a nearly complete salt rejection (>99.9%). This study addresses the pore wetting and declines in the permeate flux of the membrane distillation (MD) application in the treatment of saline oily water by implementing scalable, cost-efficient, and eco-friendly approaches.

Keywords: Hydrophilicity; Underwater superoleophobicity; Hot-pressing; Dual-layer; DCMD.

Contents

1. Introduction 3
2. Experimental 5
2.1. Materials and chemicals 5
2.2. Membrane fabrication process 6
2.3. Characterization 6
2.4. DCMD process 7
3. Results and discussion 8
3.1. Morphology 8
3.2. Porosity and thickness 11
3.3. Wettability 12

3.4. DCMD 16
4. Conclusion 20
Declaration of competing interest 20
Acknowledgment 20
Appendix A. Supplementary data 21
References 21

1. Introduction

Saline wastewater production has increased in recent decades due to considerable development in varied industries [1,2]. Wastewater treatment can be done using methods like physicochemical processes, aerobic treatment, anaerobic digestion, and membrane separation technologies [3-6]. Considering membrane-based separation, the membrane distillation (MD) process has been regarded as a next-generation, sustainable approach to treating hypersaline waters. The MD is a non-isothermal process that uses a porous hydrophobic membrane to direct hot water vapor to produce pure water [7,8]. Interestingly, MD can make full use of inexpensive heat resources to supply clean water and due to its operational condition, it will not be influenced by the quality of wastewater, making it a sought-after technology for desalination and wastewater treatment [9-13].

Surface fouling and pore wetting are however the downsides of the MD process due to the complex composition of hypersaline wastewaters [14]. In general, membrane performance can be detrimentally affected by fouling [15-17]. Severe reduction in membrane permeation because of foulant accumulation on/in the membrane can be followed by pore wetting and worsening of treated water quality [18,19]. Although the MD process experiences lower fouling compared to the pressure-driven membrane processes, the MD membranes are vulnerable to oil due to strong hydrophobic-hydrophobic interaction [20]. Low-surface-energy materials like surfactants can also increase the pore wetting of the MD membrane. These contaminants can easily invade the

78 membrane pores and render the membrane more hydrophilic which will lead to the failure in
79 rejecting salts [21-23].
80 To tackle the problem of traditional MD membranes, the concept of dual-layer structure including
81 hydrophilic/hydrophobic design has been proposed to reduce fouling and wetting [24,25]. As dual-
82 layer structures have two layers with hydrophilic and hydrophobic characteristics, researchers
83 called them the Janus membranes after the imaginary Greek god with two faces [26]. The
84 hydrophilic layer of a dual-layer structure can be fabricated by coating with hydrophilic materials
85 [27], electrospinning [28], electrospraying [29], and film casting using non-solvent-induced phase
86 separation (NIPS) [30] to form a hydrophilic or even superhydrophilic top layer with superior
87 underwater oil repellency. The hydrophobic/superhydrophobic or even omniphobic support layer
88 can also be applied to reject salts to avoid pore wetting, while the hydrophilic top layer reduces
89 fouling.
90 The robustness of the top layer is of vital importance in using dual-layer membranes.
91 Delamination or removal of the top layer during the MD process allows oil droplets to attach to
92 the membrane surface and reduce the permeate flux [31]. It also causes a severe reduction in
93 rejection because of pore wetting. Another issue is the environmental concern for using
94 hydrophilic materials, fluoroalkyl silanes, and also the complexity of the membrane fabrication
95 process. From an industrial point of view, a fabrication process should be time-efficient and as
96 simple as possible with a considerably lower production cost for both applied materials and the
97 fabrication process.
98 In this study, a practical dual-layer structure was fabricated using inexpensive polyacrylonitrile
99 (PAN) and styrene-acrylonitrile (SAN) polymers. To make the fabrication process more
100 productive and less time-consuming, a modified version of the conventional electrospinning,

electroblowing process was used. The electroblowing or air-assisted electrospinning process makes use of dry airflow to boost the fiber production rate [32,33]. The PAN polymer and its nanofibers are intrinsically hydrophilic but not hydrophilic enough to be used as a decent top layer for reducing oil fouling. The surface hydrophilicity was impressively improved using a fast-hot-pressing process. The fabricated structure turned from a spongy and soft structure to a dense and firm structure that: 1) reduced the chance of top-layer detachment during the direct contact MD (DCMD) process, 2) decreased the hydrophobicity of the surface to sufficiently reduce underwater interaction between membrane surface and oil droplets, 3) minimized the carbon footprint resulted from the application of different materials that are currently applied to make more hydrophilic surfaces. The membrane fabrication process was also eco-friendly because of the use of dimethyl sulfoxide (DMSO) as the solvent during the electroblowing process. To our knowledge, this is the first report of constructing an underwater superoleophobic and in-air highly hydrophilic dual-layer structure for the MD process using a straightforward hot-pressing process without any excessive post or pre-modification processes.

2. Experimental

2.1. Materials and chemicals

Commercial PAN polymer was purchased from the Isfahan Textile Co, Iran. Commercially available SAN polymer (SAN-4) was purchased from Ghaed Basir Co., Iran. DMSO, acetone, NaCl, and isopropyl alcohol (IPA) (extra-pure grade) were provided by Amertat Shimi, Co, Iran. Ctyltrimethylammoniumbromide (CTAB) and sodium dodecyl sulfate (SDS) were purchased from Merck, Germany. A commercial non-woven fabric made of polypropylene (PP) polymer was used

as support for nanofiber collection during the electroblowing process. Gasoline was provided by a local supplier.

2.2. Membrane fabrication process

The neat dual-layer PAN/SAN nanofibrous membrane was fabricated using PAN/DMSO + acetone (80 wt% DMSO and 20 wt% acetone; 8 wt% PAN) and SAN/DMSO + acetone (70 wt% DMSO and 30 wt% acetone; 17.5 wt% SAN) spinning solutions. Also, a small amount of CTAB salt was added to the spinning solution to reduce bead-on-string nanofibers. The electroblowing condition is summarized in Table 1. A co-axial electroblowing needle and syringe were attached via a polyethylene (PE) tube. With the help of a dry air flow, a continuous nanofiber jet was formed on the PP non-woven mat. First, a nanofibrous SAN layer was fabricated and then a nanofibrous PAN layer was fabricated on the support SAN layer. After completing the electroblowing process, the neat PAN/SAN nanofibrous membrane (designated as PAN/SAN) was immediately hot-pressed (H-PAN/SAN) under 2000 psi pressure at a temperature of 85 ℃ for 30 s to improve the physical integrity of the produced dual-layer nanofibrous membrane. A single-layer SAN nanofibrous membrane (designated as SAN) was also fabricated and hot-pressed (designated as H-SAN) to form a more uniform structure.

Table 1. Process parameters of the electroblowing process.

Nanofibrous layer	Voltage (kV)	Working distance (cm)	Polymer injection rate (μL/min)	Air flowrate (NL/min)	Spinning time (min)
PAN	22	30	90	2.5	45
SAN	18	30	90	2	45

2.3. Characterization

Surface morphology of the prepared nanofibrous layers and cross-sectional images of PAN/SAN nanofibrous membrane were observed by scanning electron microscopy (SEM, AIS 2100C, Korean Republic). The dual-layer H-PAN/SAN membrane was fractured in liquid nitrogen before the SEM test. Fiber diameter was measured by Digimizer software, and the average value of 100 fiber diameters was reported.

The thickness of the samples was measured using an accurate micrometer and cross-sectional images. The mean value of the three tests was reported as the mean thickness value.

The porosity was evaluated using the gravimetric method. First, membrane tickets were heated at 80 ℃ using a digital oven for 4 h to remove moisture and then weighed to determine the samples' dry weight. For the next step, pre-dried samples were submerged in IPA and reweighed. A full description of the process can be found in Zhou et al. [34].

The surface hydrophobicity of the prepared samples was determined by measurement of the water contact angle (WCA) using a drop shape analyzer device (KRUSS analyzer-G10 Drop Shape Analyzer, Germany). The underwater oleophobicity of the fabricated samples was measured by underwater oil contact angle (UOCA) using the same device.

The pore size of the single-layer SAN and dual-layer PAN/SAN membranes were measured using a lab-made bubble-point set-up. See Niknejad et al. [35] for more information.

The liquid entry pressure (LEP) of water was evaluated by a homemade set-up. Briefly, a circular-shaped sample of the dual-layer PAN/SAN and single-layer SAN membranes were placed between semi-cell modules. Pressure (kPa) was gradually increased to the point where the first deionized (DI) water droplet was observable on the membrane surface, and this pressure was regarded as the LEP value. The mean value of the three tests using independent membranes was reported.

2.4. DCMD process

A lab-scale DCMD set-up was used to evaluate the prepared membranes for saline and saline oily feeds. The representation of the DCMD device can be found in Bonyadi et al. [36]. The synthetic saline oily water was prepared by adding 1 g gasoline and 35 g NaCl to the DI water using a high-speed blender (rotating speed, 5000 rpm; mixing time, 1 h). Feed and permeate temperatures were 60 ± 1 ℃ and 25 ± 1 ℃, respectively. Feed and permeate streams were both set at 0.48 L/min. The feed water was mixed every 2 hours using the blender for about 5 minutes to ensure that the oil dispersion was uniform when it comes in contact with the active side of the membrane (hydrophilic layer). Also, the components of the DCMD set-up were mostly made from polyurethane (pipes) and polyethylene (feed tanks and membrane module). Therefore, the saline oily feed was circulated at least three times before starting the DCMD tests using a pump to ensure that the oil adhesion on the equipment was kept at a minimum during the DCMD tests to ensure a more accurate result. The mass and quality of the purified water were regularly monitored using a digital balance and an electrical conductivity (EC) meter, respectively. By knowing the active membrane surface area (m^2), the period of the recorded weight (h), and the amount of added water into the permeate tank (kg), the permeate flux (kg/m^2 h) could be determined.

3. Results and discussion

3.1. Morphology

The surface morphology of the top and bottom layers of the PAN/SAN membrane and the cross-sectional SEM image of the H-PAN/SAN membrane are shown in Fig 1. It is noteworthy that the morphology of the single-layer SAN was the same as the bottom layer of the PAN/SAN

membrane, as they were fabricated and hot-pressed under the same operating conditions. Therefore, only one SEM image is presented.

The polymer concentration in the dope solution is one of the deciding factors of the electrospinning process. For example, under the same electrospinning parameters, using dope solutions with low polymer concentrations will lead to the formation of cup-like defects and beaded fibers. However, raising the polymer concentration might result in a fiber diameter increase [37,38]. Therefore, the desirable morphology for the nanofibers can be obtained by controlling the polymer concentration. As observed, a defect-free nanofibrous SAN substrate with 3D microporous interconnected networks was fabricated with a suitable polymer concentration and CTAB addition to the dope solution [39]. For the PAN top layer, to maintain a balance between defects and fiber diameter enhancement, a microporous dense interconnected with minimal defects was fabricated by choosing the suitable polymer concentration.

For the dual-layer membrane, the mean fiber diameter of the neat SAN, hot-pressed SAN, neat PAN, and hot-pressed PAN was measured as 431 ± 58, 453 ± 32, 157 ± 48, and 174 ± 34 nm, respectively. Throughout the hot-pressing process, the mean fiber diameter was essentially constant because the temperature, pressure, and duration were not high enough to lead to an increase in fiber diameter while they were sufficient to increase fiber density by effectively compacting more nanofibers in a specific area [40]. Fig S1 Shows the cross-sectional SEM image for the H-PAN/SAN membrane after sonication to prove the robustness of the formed layer.

Visible changes in the pore size of the membranes can be observed after the hot-pressing process (Table 2). The hot-pressed samples had a smaller mean pore size compared to the neat membranes, which is evident by the naked eye. The cross-section image shows that the PAN and SAN layers are closely bonded with no signs of delamination at the PAN/SAN interface (Fig 1). This can be

attributed to the effective hot-pressing and the residual DMSO in the nanofibers, which further facilitate the adhesion at the PAN/SAN interface and reduces the probability of layer delamination.

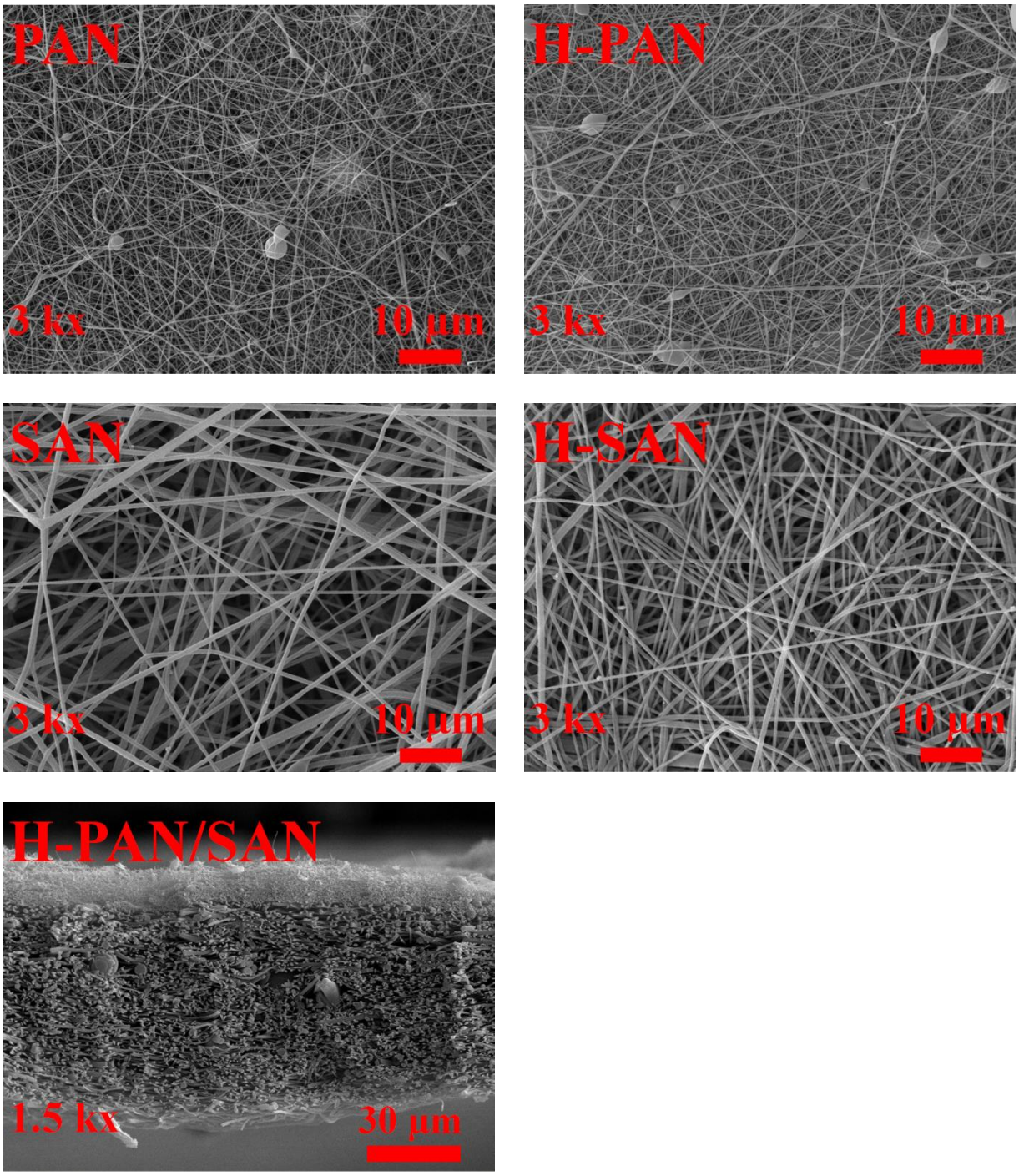

Fig 1. The surface morphology of the top layer, the bottom layer, and also the cross-section morphology of the fabricated PAN/SAN and H-PAN/SAN membranes. The SEM images' magnification with their scale bar is also presented.

3.2. Porosity and thickness

Electrospun nanofibrous membranes typically have higher porosities when compared to membranes fabricated via other membrane fabrication methods [35]. A membrane fabricated via the electroblowing process has a higher porosity than a membrane fabricated via the conventional electrospinning process (>95%). Moreover, using a longer spinning duration and a PP nonwoven mat while the charge density is kept constant can assist in making the fabricated membrane more porous by increasing the resistance against the electrical charge [41].

Higher porosity is favorable as permeability correlates positively with the porosity of the applied membrane in the MD process due to trapped air in the membrane pores that act as an insulator, thus reducing the heat loss by conduction and the water vapors having more space to pass through as a result of an increase in mean free path [35]. However, the downside is that these membranes have a larger pore size, loose and random fiber structure, wider pore size distribution, and insufficient mechanical strength that makes them inapplicable in the MD process [32]. After the hot-pressing process, the porosity of the membranes showed a declining trend. The porosity for neat SAN and PAN/SAN membranes dropped from 97.8 ± 2% and 95.7 ± 2% to 78.5 ± 1% and 75.4 ± 1%, respectively. This result is also in conformity with the declining trend reported by Yao et al. [42].

Table 2. Thickness, δ; porosity, ε; mean pore size, r_{mean}; maximum pore size, r_{max}; water contact angle, WCA; liquid entry pressure, LEP of the fabricated membranes.

Membrane	δ (µm)	ε (%)	r_{mean} (µm)	r_{max} (µm)	WCA (°)	UOCA (°)	LEP (kPa)
SAN	540 ± 50	97.8 ± 2	1.64 ± 0.03	4.12 ± 0.04	147.1 ± 1	76.2 ± 1	41.1 ± 2
H-SAN	64 ± 3	78.5 ± 1	0.43 ± 0.02	0.91 ± 0.02	142.3 ± 1	70.4 ± 1	120.3 ± 2
PAN/SAN	845 ± 50	95.7 ± 2	0.58 ± 0.02	1.32 ± 0.01	112.2 ± 1[a] 147.1 ± 1[b]	122.5 ± 1	65.3 ± 2
H-PAN/SAN	77 ± 3	75.4 ± 1	0.27 ± 0.01	0.52 ± 0.02	37.5 ± 1[a] 141.7 ± 1[b]	158.1 ± 1	156.2 ± 2

[a] top layer WCA
[b] bottom side WCA of SAN layer

Membrane thickness is another important parameter that affects the permeate flux, mechanical properties, and salinity the membrane can efficiently handle. The increase in salinity causes a drop in feed vapor pressure, consequently, if the transmembrane temperature is not high enough the loss in energy efficiency becomes considerable [43]. Although thicker membranes have higher energy efficiency, the driving force is insufficient to fully boost permeation. These membranes are preferable in the treatment of highly saline waters due to possible mass transfer resistance and a lower permeate flux [44,45]. Therefore, to achieve higher rejection and permeate flux, it is essential to determine a suitable balance between porosity and thickness. The thickness value for the neat SAN and PAN/SAN membranes reduced from 540 ± 50 and 845 ± 50 µm to 64 ± 3 and 77 ± 3 µm for the H-SAN and H-PAN/SAN, respectively. The porosity and thickness of the fabricated membranes show that the hot-pressed membranes have lower porosity and thickness values compared to the neat samples [42]. Thus, the permeability and rejection can be enhanced through a straightforward hot-pressing process [32].

3.3. Wettability

One of the major obstacles to the universality of MD is membrane wetting. The wetting phenomenon starts with the larger pores, and then gradually spreads throughout the whole membrane. Therefore, a larger maximum pore size is not favorable. While the pore size range applicable for MD membranes is between 0.1 and 1 µm, the preferred pore size for membranes applied for the MD process is reported to be in the range of 0.2 - 0.5 µm [12,46]. There are several factors to assess the wetting tendency of a membrane during the MD process such as WCA, maximum pore size, and LEP, which will be discussed later in this section. Moreover, the relationship of WCA, maximum pore size, and LEP is governed by the Laplace-Young equation ($LEP= -(\beta\gamma_1 \cos \theta)/r_{max}$) [47]. In simpler terms, to fabricate an optimal membrane, a balance between the abovementioned factors must be met. A membrane suitable for MD application should have a higher WCA, smaller maximum pore size, and a higher LEP value [48]. However, a hydrophobic membrane in the presence of oil in the saline feed is prone to pore blockage and pore wetting due to the hydrophobic-hydrophobic interaction between the oily content and the membrane surface. Therefore, the top layer that is in contact with the saline oily feed should be oleophobic enough to prevent pore blockage and wetting by forming a hydration layer at the membrane feed interface [20,49].

The WCA and UOCA values of the fabricated membranes are tabulated in Table 2 and related images are shown in Fig 2. Surface hydrophobicity can be manipulated by altering surface roughness using various methods [50,51]. It is worth stating that membranes fabricated via the electrospinning process (using hydrophobic polymers) have intrinsically higher WCA compared to membranes fabricated via other methods (i.e., NIPS). This can be ascribed to the non-woven nature of the fabricated membranes, which elevates surface roughness to form a re-entrant structure [52]. The WCA for the neat and H-SAN was measured as 147.1 ± 1° and 142.3 ± 1°,

respectively. Since the surface energy is constant, the reduction can be attributed to a decrease in surface roughness caused by the hot-pressing process [32,42]. Additionally, the WCA for the bottom layer of the PAN/SAN membrane was measured as 147.1 ± 1° and 141.7 ± 1° for neat and hot-pressed ones, respectively. It is essentially the same as the H-SAN membrane since they were fabricated and hot-pressed under the same parameters. The WCA for the top layer of the neat and hot-pressed PAN/SAN membranes was measured as 112.2 ± 1° and 37.5 ± 1°, respectively. This sharp decline can be ascribed to the highly rough surface of the neat PAN membrane that increases the amount of trapped air underneath the membrane. Moreover, the reported WCAs in Table 2 were measured immediately after placing a water droplet on the surface. Once the hot-pressing process was applied, surface roughness was reduced to considerably boost hydrophilicity. In addition, UOCA was improved from 122.5º for the PAN/SAN membrane to 158.1º for the H-PAN/SAN membrane. So, the oil repellency of the top layer underwent substantial enhancement by simply employing the hot-pressing process. A film showing the behavior of a gasoline droplet when contacting the top surface of the H-PAN/SAN is provided as supporting data (Video S1).

As mentioned previously, the existence of large pores may lead to partial pore wetting which will eventually lead to total wetting. Therefore, a hot-pressing process can significantly enhance the wetting resistance of the fabricated membrane. As seen in Table 2, the maximum pore size for the neat SAN and the neat PAN/SAN membrane decreased from 4.12 ± 0.04 and 1.32 ± 0.01 µm to 0.91 ± 0.02 and 0.52 ± 0.02 µm, respectively. The reported values are in the favorable range reported by Pan et al. [46]. The largest maximum pore size and mean pore size were measured for the neat SAN membrane, which results in a larger fiber diameter with a fluffy structure of the fabricated membrane. The smallest pore size was for the hot-pressed PAN/SAN membrane due to its compact structure.

The LEP value is the minimum transmembrane pressure exerted that will lead to the liquid feed overcoming the repellency of the hydrophobic surface and wetting the pores. [49] LEP value is one of the most important determining factors indicating the wetting resistance of the fabricated membranes because higher LEP values can guarantee a superior anti-wetting performance throughout the MD process. Table 2 demonstrates that higher LEP values have a better anti-wetting performance for the fabricated membranes. For the hot-pressed membranes compared to the corresponding neat membranes, the LEP value increased considerably. The LEP value for the neat SAN and neat PAN/SAN membranes increased from 41.1 ± 2 and 65.3 ± 2 kPa to 120.3 ± 2 and 156.2 ± 2 kPa for the H-SAN and H-PAN/SAN membrane, respectively. This can be attributed to a decline in the maximum pore size because they are inversely correlated according to the Laplace-Young equation [53,54].

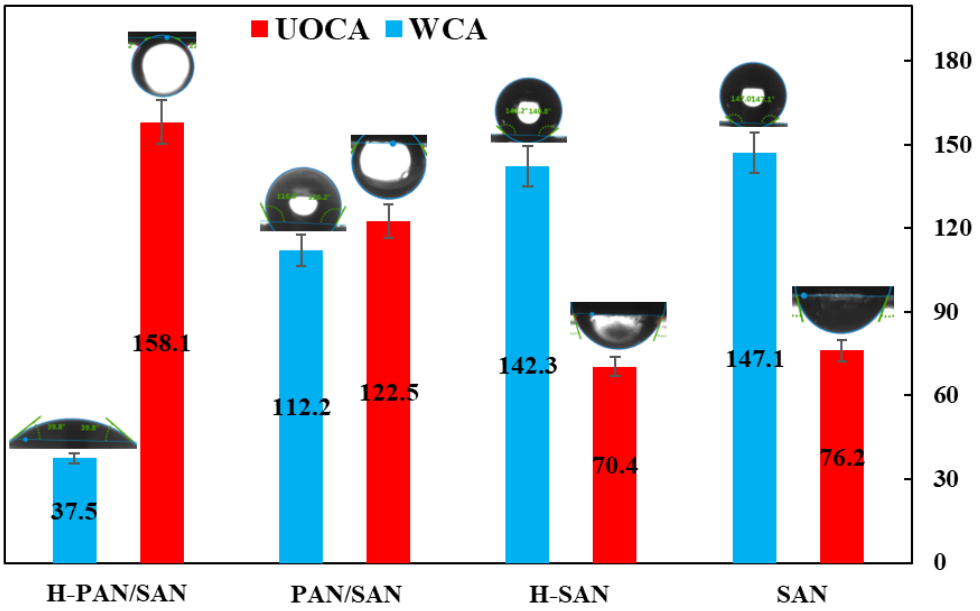

Fig 2. A diagram showing the in-air WCA and UOCA measurements for the used membranes in this study. The top layer of the membranes was used to measure these values. As an example, in-

air WCA for H-PAN/SAN was measured by placing DI water on the top of the membrane (PAN nanofibrous layer). To measure UOCA using the same membrane, it was immersed in water to contact the gasoline droplet to the top layer. Video S1 clearly shows how UOCA tests were performed.

3.4. DCMD

DCMD performance of the H-SAN and H-PAN/SAN membranes using saline water and oily saline water as a feed was thoroughly investigated. The neat membrane was not further assessed due to low mechanical strength (see ref. [52]), large maximum pore size (>1 µm, see Table 2), low LEP value, as well as high thickness [32]. It is a well-known fact that the existence of contaminants in the feed water can lead to partial wetting or pore blockage of the membrane, which will adversely affect MD performance [55,56]. Due to the composition of the saline oily feed, the wetting phenomena can be identified by observing the water conductivity in the permeate. The DCMD operating condition such as temperature difference (ΔT = 35 °C), feed concentration, and permeate flow rates (0.48 L/min) were kept constant during the 24 h test.

Fig 3 shows flux-time and conductivity-time profiles for the hot-pressed SAN and H-PAN/SAN membranes using saline water (Fig 3-A) and oily saline water (Fig 3-B) as a feed. Using the saline feed, a mean permeate flux of 42.26 and 34.89 kg/m^2 h was measured for the H-SAN and H-PAN/SAN, respectively. The H-SAN membrane achieved a higher flux compared to the dual-layer H-PAN/SAN membrane in saline water. The lower permeate flux for the H-PAN/SAN membrane can be attributed to the additional mass transfer resistance of the PAN top layer. The final EC value for the tested membranes did not exceed 5 µS/cm. The EC value showed no sign of membrane wetting in both cases since it does not demonstrate a rising trend. Also, both membranes

demonstrated high rejection (>99.9%) without a decline in permeate flux during the DCMD process due to high hydrophobicity and a proper LEP value.

Fig 3-B shows the DCMD performance of the membranes for treatment of the saline oily feed. In the presence of oil, the H-PAN/SAN membrane showed a high rejection (>99.9%), without a decline in permeate flux during the DCMD process, while in the case of the single-layer H-SAN membrane, the permeate flux sharply dropped due to pore blockage caused by the hydrophobic-hydrophobic interaction. Moreover, the adsorption of oil can increase the probability of pore wetting [57]. The membrane wetting is confirmed by the increase in EC value depicted in Fig 3-B. The mean permeate flux for the H-PAN/SAN membrane was 32.80 kg/m^2 h, which shows a 6% reduction in the permeate flux when compared to the saline water. This flux reduction can be caused by the formation of an oily layer that restricts the evaporation area [58]. The salt rejection of the H-PAN/SAN membrane also demonstrated the effect of a strong hydration layer between the membrane and oil droplets.

Fig 4 shows the DCMD performance of the H-PAN/SAN membrane for treating SDS-including saline oily feed (SDS concentration, 0.2 mM; salt concentration, 35 g/L; gasoline concentration, 1 g/L). Permeate flux and salt rejection were measured as 31.97 ± 2 kg/m^2 h and >99.9%, respectively, during 9 h continuous test. Applied DCMD conditions were the same as the previous tests (Temperature differences. 35 ℃; feed and permeate flow rates, 0.48 L/min). A negligible reduction in permeate flux was observed due to temporary fouling by smaller oil droplets. However, superior under water oil repellency of the H-PAN/SAN membrane by creating a strong hydration layer made a proper barrier for reversable fouling of oil droplets as these small oil particles can join together to form a bigger oil droplet to detach easily for the surface. Also,

363 tight pore size of the nanofibrous PAN layer can help to repel oil droplets to keep DCMD process
364 going.
365 A literature survey of recent work regarding dual-layer membranes is provided in Table 3. The
366 tabulated works were used for saline oily water treatment using the DCMD process. The salt (35
367 g/L) and oil concentrations (1 g/L crude oil expect for this work) were the same when compared
368 to the reported results. The H-PAN/SAN membrane was comparable with the literature
369 considering UOCA. Due to the superior hydrophilicity of the PAN top layer in the dual-layer
370 structure, a superoleophobic surface was observed. It can sufficiently repel oil droplets to keep the
371 DCMD performance at a good level (i.e., high salt rejection without any change in flux).
372 Considering environmental issues and cost-effectiveness, the proposed dual-layer membrane
373 outperforms the other membranes by using a straightforward and eco-friendly hot-pressing, low-
374 toxic DMSO solvent, productive electroblowing process, and low-priced membrane materials.
375

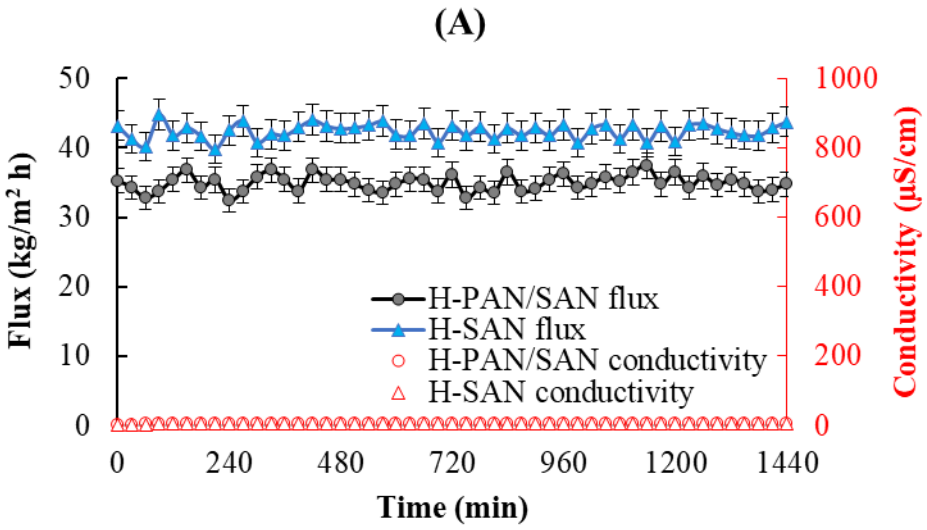

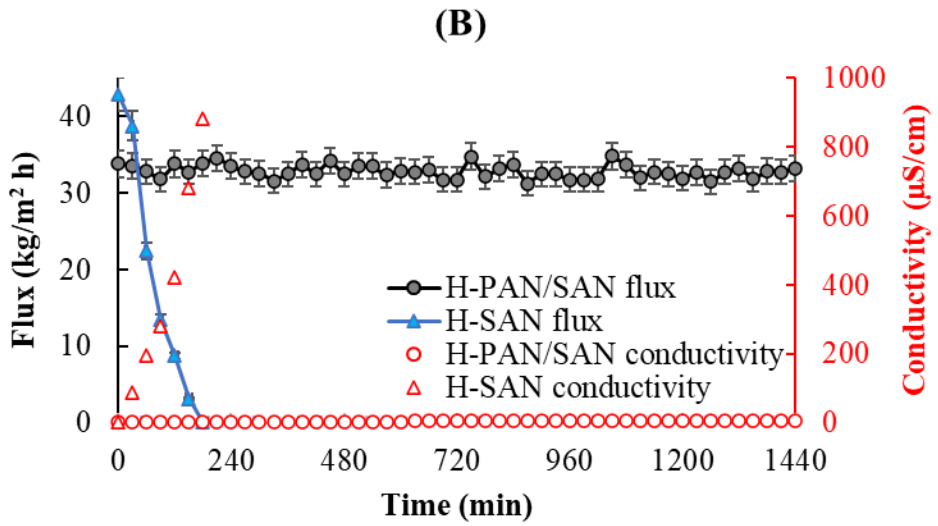

376 Fig 3. DCMD performance of the H-SAN and H-PAN/SAN using (A) saline water (35 g/L NaCl)
377 and (B) oily saline water as feed. The temperature of feed and permeate were 60 ± 1 and 25 ± 1
378 ℃, respectively. Moreover, the flow rate of 0.48 L/min was applied to the feed and permeate sides.
379

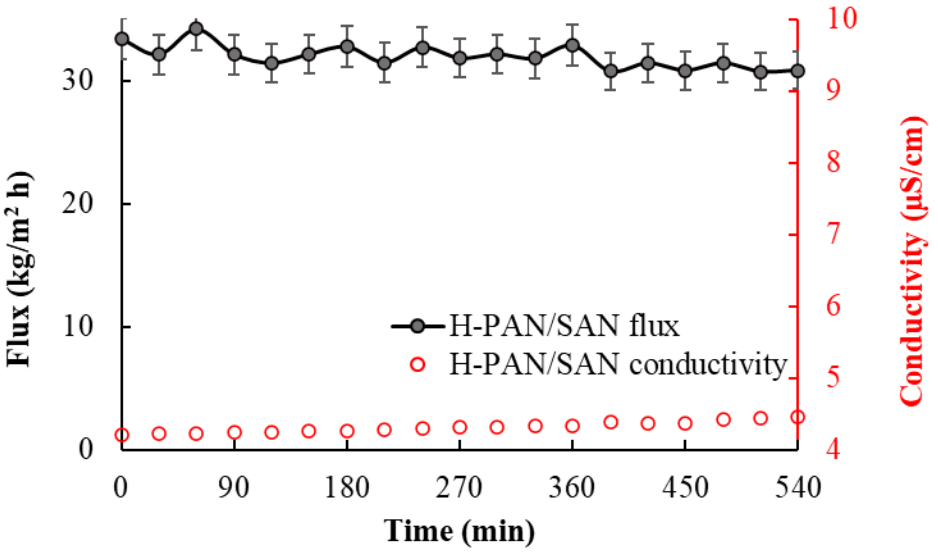

380
381 Fig 4. DCMD performance of H-PAN/SAN membrane for treating SDS-including saline oily
382 water feed solution. Temperature difference and feed/permeate flow rate were set at 35 ℃and 0.48
383 mL/min, respectively.

Table 3. Physical characteristics and DCMD performance of recently published flat-sheet membranes for saline oily treatment (35 g NaCl + 1 g oil/L).

Membrane	UOCA (°)	ε (%)	r_{mean} (µm)	δ (µm)	LEP (kPa)	Flux (kg/m^2 h)	ΔT (°C)	t_{DCMD} (h)	R (%)	Reference
Janus NFMs	164	-	1.45	66	136.0	25.4	40	30	100	[29]
Modified PVDF	149.5	72.5	0.38	180.1	326	26.1	40	36	100	[18]
PTFE/PAN-OH	161.7	69.8	0.21	267.8	375	15.2	33	25	~100	[59]
CTS/PFO-PVDF	>130	-	-	177.5	300	27.0	40	36	99.9	[60]
PTFE/PVA-Si-GA	156.5	41.6	0.41	348.0	-	17.5	33	50	100	[20]
PTFE/CA-SiNPs	154.2	50.6	0.47	303.0	-	~19.9 [a]	33	30	-	[28]
PTFE-9CA	158	62.5	0.21	248	371	16.85	33	18	100	[61]
H-PAN/SAN	158.1	75.4	0.27	77	156.2	32.80	35	24	>99.9	Current work

[a] Initial flux

4. Conclusion

For the treatment of saline oily water by DCMD, an eco-friendly and inexpensive PAN/SAN membrane was fabricated. In order to boost the production rate, the electroblowing process was implemented using a low-toxic DMSO solvent to fabricate a dual-layer PAN/SAN membrane. Then, through a simple hot-pressing process, the membrane characteristics including a decrease in surface hydrophobicity and an increase in the LEP value were manipulated in a way to meet the demands of the MD process. Interaction between oil and the hydrophobic surface was mitigated by a layer of PAN nanofibers. As the PAN layer of the hot-pressed PAN/SAN membrane became underwater superoleophobic, nearly complete salt rejection without any considerable increase in EC value was measured while for the hot-pressed single-layer SAN membrane, the wetting started from the beginning of the DCMD process. It is hopeful that the anti-wetting and anti-fouling properties of the fabricated membrane can address the challenging issue of saline oily water treatment in a more scalable, eco-friendly, and cost-efficient manner.

Declaration of competing interest

The authors declare that they have no known competing financial interests or personal relationships that could have appeared to influence the work reported in this paper.

Acknowledgment

This work is dedicated to my father (Bahram Sallakh Niknejad) who backed me a lot during the past years. He is the sole provider of my published papers (11 papers) and I enjoy having him on my side.

Appendix A. Supplementary data

Cross-sectional morphology of sonicated H-PAN/SAN membrane is also provided in Fig S1. A video showing the nonstick character of the H-PAN/SAN membrane against gasoline was also provided in video S1.

References

[1] V. Karanikola, C. Boo, J. Rolf, M. Elimelech, Engineered slippery surface to mitigate gypsum scaling in membrane distillation for treatment of hypersaline industrial wastewaters, Environ. Sci. Technol. 52 (2018) 14362–14370.

[2] Y. Xu, J. Ma, D. Liu, H. Xu, F. Cui, W. Wang, Origami system for efficient solar driven distillation in emergency water supply, Chem. Eng. J. 356 (2019) 869–876.

[3] M.C. Tomei, V. Stazi, D.M. Angelucci, Biological treatment of hypersaline wastewater in a continuous two-phase partitioning bioreactor: analysis of the response to step, ramp and impulse loadings and applicability evaluation, J. Clean. Prod. 191 (2018) 67–77.

[4] B. Alkotaini, S.L. Tinucci, S.J. Robertson, K. Hasan, S.D. Minteer, M. Grattieri, Alginate-encapsulated bacteria for the treatment of hypersaline solutions in microbial fuel cells, Chembiochem 19 (2018) 1162–1169.

[5] S.F. Corsino, M. Capodici, M. Torregrossa, G. Viviani, Physical properties and extracellular polymeric substances pattern of aerobic granular sludge treating hypersaline wastewater, Bioresour. Technol. 229 (2017) 152–159.

[6] R. Zhang, J. Tian, S. Gao, B. Van der Bruggen, How to coordinate the trade-off between water permeability and salt rejection in nanofiltration? J. Mater. Chem. A 8 (2020) 8831–8847.

[7] G. Zuo, R. Wang, Novel membrane surface modification to enhance anti-oil fouling property for membrane distillation application. J. Membr. Sci. 447 (2013) 26-35.

[8] L.D. Tijing, Y.C. Woo, J.S. Choi, S. Lee, S.H. Kim, H.K. Shon, Fouling and its control in membrane distillation - A review. J. Membr. Sci. 475 (2015) 215-44.

[9] M.S. El-Bourawi, Z. Ding, R. Ma, M. Khayet, A framework for better understanding membrane distillation separation process, J. Membr. Sci. 285 (2006) 4–29.

[10] A.K. An, J. Guo, S. Jeong, E.J. Lee, S.A.A. Tabatabai, T. Leiknes, High flux and antifouling properties of negatively charged membrane for dyeing wastewater treatment by membrane distillation, Water Res. 103 (2016) 362–371.

[11] C. Su, T. Horseman, H. Cao, K. Christie, Y. Li, S. Lin, Robust superhydrophobic membrane for membrane distillation with excellent scaling resistance, Environ. Sci. Technol. 53 (2019) 11801–11809.

[12] A. Alkhudhiri, N. Darwish, N. Hilal, Membrane distillation: a comprehensive review, Desalination 287 (2012) 2–18.

[13] Z. Xiao, R. Zheng, Y. Liu, H. He, X. Yuan, Y. Ji, D. Li, H. Yin, Y. Zhang, X.M. Li, T. He, Slippery for scaling resistance in membrane distillation: a novel porous micropillared superhydrophobic surface, Water Res. 155 (2019) 152–161.

[14] J.R. Werber, C.O. Osuji, M. Elimelech, Materials for next-generation desalination and water purification membranes, Nat. Rev. Mater. 1 (2016) 16018.

452 [15] D.M. Warsinger, J. Swaminathan, E. Guillen-Burrieza, H.A. Arafat, H.L.V. John, Scaling
453 and fouling in membrane distillation for desalination applications: a review, Desalination 356
454 (2015) 294–313.

455 [16] M. Rezaei, D.M. Warsinger, V.J. Lienhard, M.C. Duke, T. Matsuura, W.M. Samhaber,
456 Wetting phenomena in membrane distillation: mechanisms, reversal, and prevention, Water Res.
457 139 (2018) 329–352.

458 [17] Z. Wang, S. Lin, Membrane fouling and wetting in membrane distillation and their mitigation
459 by novel membranes with special wettability, Water Res. 112 (2017) 38–47.

460 [18] Z. Wang, D. Hou, S. Lin, Composite membrane with underwater-oleophobic surface for anti-
461 oil-fouling membrane distillation, Environ. Sci. Technol. 50 (2016) 3866–3874.

462 [19] K.R. Zodrow, E. Barzeev, M.J. Giannetto, M. Elimelech, Biofouling and microbial
463 communities in membrane distillation and reverse osmosis, Environ. Sci. Technol. 48 (2014)
464 13155–13164.

465 [20] D. Hou, C. Ding, K. Li, D. Lin, D. Wang, J. Wang, A novel dual-layer composite membrane
466 with underwater-superoleophobic/hydrophobic asymmetric wettability for robust oil-fouling
467 resistance in membrane distillation desalination, Desalination 428 (2018a) 240–249.

468 [21] X. An, Z. Liu, Y. Hu, Amphiphobic surface modification of electrospun nanofibrous
469 membranes for anti-wetting performance in membrane distillation, Desalination 432 (2018) 23–
470 31.

[22] J. Lee, C. Boo, W.H. Ryu, A.D. Taylor, M. Elimelech, Development of omniphobic desalination membranes using a charged electrospun nanofiber scaffold, ACS Appl. Mater. Interfaces 8 (2016) 11154–11161.

[23] Z. Zhu, Y. Liu, H. Hou, W. Shi, F. Qu, F. Cui, W. Wang, Dual-bioinspired design for constructing membranes with superhydrophobicity for direct contact membrane distillation, Environ. Sci. Technol. 52 (2018) 3027–3036.

[24] Y.X. Huang, Z. Wang, J. Jin, S. Lin, Novel Janus membrane for membrane distillation with simultaneous fouling and wetting resistance, Environ. Sci. Technol. 51 (2017) 13304–13310.

[25] L. Deng, P. Li, K. Liu, X. Wang, B.S. Hsiao, Robust superhydrophobic dual layer nanofibrous composite membranes with a hierarchically structured amorphous polypropylene skin for membrane distillation, J. Mater. Chem. A 7 (2019)11282–11297.

[26] S. Cong, F. Guo, Janus nanofibrous membranes for desalination by air gap membrane distillation, ACS Appl. Polym. Mater. 1 (2019) 3443–3451.

[27] K. Wang, D. Hou, J. Wang, Z. Wang, B. Tian, P. Liang, Hydrophilic surface coating on hydrophobic PTFE membrane for robust anti-oil-fouling membrane distillation, Appl. Surf. Sci. 450 (2018) 57–65.

[28] D. Hou, Z. Wang, K. Wang, J. Wang, S. Lin, Composite membrane with electrospun multiscale-textured surface for robust oil-fouling resistance in membrane distillation, Journal of Membrane Science, 546 (2018b) 179–187.

[29] Z. Zhu, Z. Liu, L. Zhong, C. Song, W. Shi, F. Cui, W. Wang, Breathable and asymmetrically superwettable Janus membrane with robust oil-fouling resistance for durable membrane distillation, J. Membr. Sci. 563 (2018) 602–609.

[30] M. Lou, X. Fang, Y. Liu, G. Chen, J. Zhou, C. Ma, H. Wang, J. Wu, Z. Wang, F. Li, Robust dual-layer Janus membranes with the incorporation of polyphenol/Fe3+ complex for enhanced anti-oil fouling performance in membrane distillation, Desalination 515 (2021) 115184.

[31] Z. Zhu, L. Zhong, X. Chen, W. Zheng, J. Zuo, G. Zeng, W. Wang, Monolithic and self-roughened Janus fibrous membrane with superhydrophilic/omniphobic surface for robust antifouling and antiwetting membrane distillation, J. Membr. Sci. 615 (2020) 118499.

[32] R. Sallakhniknezhad, M. Khorsi, A.S. Niknejad, S. Bazgir, A. Kargari, M. Sazegar, M. Rasouli, S. Chae, Enhancement of Physical Characteristics of Styrene–Acrylonitrile Nanofiber Membranes Using Various Post-Treatments for Membrane Distillation, Membranes 11 (2021) 969.

[33] A.S. Niknejad, S. Bazgir, A. Kargari, Mechanically improved superhydrophobic nanofibrous polystyrene/high- impact polystyrene membranes for promising membrane distillation application, J. Appl. Polym. Sci. 138 (2021a) 50917.

[34] T. Zhou, Y. Yao, R. Xiang, Y. Wu, Formation and characterization of polytetrafluoroethylene nanofiber membranes for vacuum membrane distillation, J. Membr. Sci. 453 (2014) 402–408.

[35] A.S. Niknejad, S. Bazgir, A. Sadeghzadeh, M.M.A. Shirazi, Evaluation of a novel and highly hydrophobic acrylonitrile-butadiene-styrene membrane for direct contact membrane distillation: electroblowing/air-assisted electrospraying techniques, Desalination 500 (2021b) 114893.

[36] E. Bonyadi, A.S. Niknejad, F.Z. Ashtiani, S. Bazgir, A. Kargari, A well-designed polystyrene/polycarbonate membrane for highly saline water desalination using DCMD process, Desalination 528 (2022) 115604.

[37] B. Veleirinho, M.F. Rei, J.A. Lopes-DA-Silva, Solvent and concentration effects on the properties of electrospun poly(ethylene terephthalate) nanofiber mats, J. Polym. Sci. B: Polym. Phys. 46 (2008) 460–471.

[38] B. Tarus, N. Fadel, A. Al-Oufy, and M. El-Messiry, Effect of polymer concentration on the morphology and mechanical characteristics of electrospun cellulose acetate and poly (vinyl chloride) nanofiber mats, Alexandria Eng. J. 55 (2016) 2975–2984.

[39] L. Huang, S.S. Manickam, J.R. McCutcheon, Increasing strength of electrospun nanofiber membranes for water filtration using solvent vapor, J. Membr. Sci. 436 (2013) 213-220.

[40] H. Ke, M. Feldman, P. Guzman, J. Cole, Q. Wei, B. Chu, A. Alkhudhiri, R. Alrasheed, B.S. Hsiao, Electrospun polystyrene nanofibrous membranes for direct contact membrane distillation, J. Membr. Sci. 515 (2016) 86-97.

[41] A.S. Niknejad, S. Bazgir, A. Kargari, Novel Triple-Layer HIPS/SBR/PP Nanofibrous Membranes for Robust DCMD Desalination, Ind. Eng. Chem. Res 60 (2021c) 2911–2920.

[42] M. Yao, Y.C. Woo, L.D. Tijing, W.G. Shim, J.S. Choi, S.H. Kim, H.K. Shon, Effect of heat-press conditions on electrospun membranes for desalination by direct contact membrane distillation, Desalination 378 (2016) 80–91.

[43] L. Eykens, I. Hitsov, K. De Sitter, C. Dotremont, L. Pinoy, I. Nopens, B. Van der Bruggen, Influence of membrane thickness and process conditions on direct contact membrane distillation at different salinities, J. Membr. Sci. 498 vol. 498 (2016) 353-364.

[44] L. Eykens, K. De Sitter, C. Dotremont, W. De Schepper, L. Pinoy, B. Van Der Bruggen, Wetting Resistance of Commercial Membrane Distillation Membranes in Waste Streams Containing Surfactants and Oil, Appl. Sci. 7 (2017) 118.

[45] A.S. Niknejad, S. Bazgir, A. Sadeghzadeh, M.M.A. Shirazi, Styrene-acrylonitrile (SAN) nanofibrous membranes with unique properties for desalination by direct contact membrane distillation (DCMD) process, Desalination 488 (2020) 114502.

[46] C.-Y. Pan, G.-R. Xu, K. Xu, H.-L. Zhao, Y.-Q. Wu, H.-C. Su, J.-M. Xu, R. Das, Electrospun nanofibrous membranes in membrane distillation: Recent developments and future perspectives, Sep. Purif. Technol. 221 (2019) 44–63.

[47] O. Makanjuola, F. Ahmed, I. Janajreh, R. Hashaikeh, Development of a dual-layered PVDF-HFP/cellulose membrane with dual wettability for desalination of oily wastewater, J. Membr. Sci. 570–571 (2019) 418–426.

[48] N.G.P. Chew, S. Zhao, R. Wang, Recent advances in membrane development for treating surfactant- and oil-containing feed streams via membrane distillation, Adv. Colloid Interface Sci. 273 (2019) 102022.

[49] H. Chamani, J. Woloszyn, T. Matsuura, D. Rana, C.Q. Lan, Pore wetting in membrane distillation: A comprehensive review, Prog. Mater. Sci. 122 (2021) 100843.

[50] E. Celia, T. Darmanin, E. Taffin de Givenchy, S. Amigoni, F. Guittard, Recent advances in designing superhydrophobic surfaces, J. Colloid Interface Sci. 402 (2013) 1–18.

[51] M.K. Sarkar, K. Bal, F. He, J. Fan, Design of an outstanding super-hydrophobic surface by electro-spinning, Appl. Surf. Sci. 257 (2011) 7003–7009.

[52] A.S. Niknejad, S. Bazgir, A. Kargari, M. Barani, E. Ranjbari, and M. Rasouli, A high-flux polystyrene-reinforced styrene-acrylonitrile/polyacrylonitrile nanofibrous membrane for desalination using direct contact membrane distillation, J. Membr. Sci. 638 (2021d) 119744.

[53] G. Rácz, S. Kerker, Z. Kovács, G. Vatai, M. Ebrahimi, P. Czermak, Theoretical and experimental approaches of liquid entry pressure determination in membrane distillation processes, Periodica Polytech., Chem. Eng. 58 (2014) 81–91,

[54] Y. Liao, C.H. Loh, R. Wang, A.G. Fane, Electrospun superhydrophobic membrane with unique structure for membrane distillation, ACS Appl. Mater. Interfaces 6 (2014) 16035–16048,

[55] K.J. Lu, Y. Chen, T.-S. Chung, Design of omniphobic interfaces for membrane distillation—A review, Water Res. 162 (2019) 64–77.

[56] X. Du, Z. Zhang, K.H. Carlson, J. Lee, T. Tong, Membrane fouling and reusability in membrane distillation of shale oil and gas produced water: Effects of membrane surface wettability, J. Membr. Sci. 567 (2018) 199–208.

[57] M. Gryta, Resistance of Polypropylene Membrane to Oil Fouling during Membrane Distillation, Membranes 11 (2021) 552.

[58] L. Han, Y.Z. Tan, T. Netke, A.G. Fane, J.W. Chew, Understanding oily wastewater treatment via membrane distillation. J. Membr. Sci. 539 (2017) 284–294.

[59] M. Tang, D. Hou, C. Ding, K. Wang, D. Wang, J. Wang, Anti-oil-fouling hydrophobic-superoleophobic composite membranes for robust membrane distillation performance, Sci. Total Environ. 696 (2019) 133883.

[60] Z. Wang, S. Lin, The impact of low-surface-energy functional groups on oil fouling resistance in membrane distillation, J. Membr. Sci. 527 (2017) 68–77.

[61] M. Tang, K.S.S. Christie, D. Hou, C. Ding, X. Jia, J. Wang, Fabrication of a novel underwater-superoleophobic/hydrophobic composite membrane for robust anti-oil-fouling membrane distillation by the facile breath figures templating method, J. Membr. Sci. 617 (2021) 118666.